ABSTRACT

Title of Document: TIN WHISKER RISK ASSESSMENT STUDIES

Tong Fang, Doctor of Philosophy, 2005

Directed By: Professor Michael G. Pecht
Department of Mechanical Engineering

As a result of the global transition to lead (Pb)-free electronics, pure tin and high tin lead-free alloys have been widely adopted by the electronics part manufacturers as the materials of terminal finishes. However, electrically conductive tin whiskers have been found to develop in pure tin or high tin alloy finished surfaces, resulting in a reliability concern. Experimental results and observation appear to support the hypothesis that the driving forces for whisker formation is compressive stress. However, no accepted model and accelerated factors are available to describe and predict whisker growth. Though the issue of metal whiskers has been studied for over 60 years, currently there is no an industry-wide accepted methodology to quantify tin whisker risk.

In this dissertation, a tin whisker risk assessment algorithm, which mainly focuses on bridging risk, is developed. The goal of this risk assessment algorithm is to provide a practical methodology for the electronics industry to quantify the failure risks posed by tin whiskers on tin-plated electronic products. This algorithm assessES tin whisker bridging risk quantitatively as a function of time. Probabilistic and statistical methods are applied to quantify the risk parameters, such as whisker density and length, related to

assess tin whisker risk. Monte Carlo technique is the basic tool to sample the whiskers and assess the bridging risk.

Two experiments are designed and conducted to simulate bridging failures caused by fixed and broken free whiskers. The methods to collect the information of the risk parameters are demonstrated. Prediction of whisker growth and tin whisker bridging risk is conducted based on the collected information. Error analyses on the differences between simulation and experimental results are provided.

TIN WHISKER RISK ASSESSMENT STUDIES

By

Tong Fang

Dissertation submitted to the Faculty of the Graduate School of the
University of Maryland, College Park, in partial fulfillment
of the requirements for the degree of
Doctor of Philosophy
2005

Advisory Committee:
Professor Michael G. Pecht, Chair/Advisor
Professor David F. Barbe
Associate Professor Peter A. Sandborn
Associate Professor F. Patrick McCluskey
Assistant Professor Bao Yang
Dr. Michael D. Osterman

© Copyright by
Tong Fang
2005

Dedication

This volume is lovingly dedicated to my wife and partner, Ruxin Ma, our adorable child, Eric, and my mom, Lixian Qi.

Acknowledgements

First of all, I would like to genuinely acknowledge my advisor, Professor Michael Pecht, for his enlightening guidance and support. I also recognize the tin whisker study group leader, Dr. Michael Osterman, for his insightful comment and help. Special thanks go to my dissertation committee members for their suggestions and evaluations on my work.

I am grateful to many people of the faculty, the staff and my colleagues at CALCE Electronic Products and Systems Center for their valuable help and comments. I also appreciate Jay Brusse at NASA, who provided me zinc whisker for my validation experiments.

I thank Ruxin, Eric, and mom for their endless love and support.

Table of Contents

Dedication ii
Acknowledgements iii
Table of Contents iv
List of Tables vi
Chapter 1 Introduction of Tin Whiskers 1
1.1 A Brief Description of Lead-free Movement 1
1.2 Attributions of Tin Whiskers 2
1.3 Whisker Formation and Growth Mechanisms 5
1.4 Effects of Environmental Factors on Whisker Growth 9
1.5 Mitigation Strategies 10
1.6 History Research on Tin Whiskers 14
Chapter 2 Problem Statement, Dissertation Objectives and Scope 12
2.1 Overview of the Risks Associated with Tin Whiskers 12
2.2 Field Failures Caused by Whiskers 20
2.3 Previous Efforts to Quantify Bridging Risks Associated with Tin Whiskers 23
2.3.1 Pinsky's risk assessment algorithm 23
2.3.2 Okada's reliability approach model 29
2.4 Motivation of this Research 30
2.5 Objectives of this Research 31
2.6 Scope of this Research 31
2.7 Description of this Dissertation 31
Chapter 3 Whisker Growth Analysis 33
3.1 Electronics Industry's Acceptance Level for Whisker Growth 33
3.2 General Description of the Experimental Study 34
3.3 Whisker Density 36
3.4 Whisker Length 37
3.5 Whisker Growth Angle 41
3.6 Whisker Growth Rate 42
3.7 Summaries of Whisker Growth 44
Chapter 4 Development of Tin Whisker Assessment Algorithm 45
4.1 Fundamental Elements of the Risks Assessment Algorithm 45
4.1.1 Risk categorization 45
4.1.2 Risk parameters 46
4.1.3 Distributions of whisker growth parameters and characteristic parameters 47
4.2 Risk Assessment for Fixed Whiskers 48
4.2.1 Failure definition 48
4.2.2 Whisker growth parameters and their distributions 49
4.2.3 Procedure to quantify fixed bridging risk in terms of probability 49
4.2.4 Procedure to quantify risk in terms of bridging number 52
4.2.5 An example of implementation for fixed risk 54
4.3 Risk Assessment for Free Whiskers 59
4.3.1 Failure definition 60

4.3.2 Characteristic parameters related to free whiskers 60
4.3.3 Assessment algorithm to quantify bridging risk in terms of risk probability ……………………………………………………………………………..61
4.3.4 Assessment algorithm to quantify risk in terms of bridging number for free whiskers 63
4.3.5 An example of implementation for free whiskers...................................... 65
4.4 Integration of Fixed and Free Risks... 69
4.5 Effectiveness of Mitigation Strategies and Cost 69
Chapter 5 Simulation Experiments 71
5.1 Experimental Design for Fixed Failure Risk 71
5.1.1 Experimental vehicles and conditions 71
5.1.2 Results of the experiment.. 73
5.2 Experimental Design for the Free Risk.. 79
5.2.1 Experimental vehicles.. 79
5.2.2 Design of data collection 80
5.2.3 Experimental and simulation results... 81
5.2.4 Error analysis 82
Chapter 6 Conclusions and Summary 84
Chapter 7 Contributions and Recommendations 86
7.1 Contributions of This Work 86
7.2 Recommendations for the Future Work 87
7.2.1 Probability of occurrence of an electrical short 88
7.2.2 Bridging risk simulation on a real electronic system.................................. 88
7.2.3 Risk assessment algorithm development to quantify the other two risks.... 91
Bibliography 92

List of Tables

Table 2.1 Risk factors 27
Table 2.2 Simulated values of risk factors and the results 28
Table 3.1 iNEMI's whisker length limits 34
Table 3.2 Results of the three measurements on whisker density 36
Table 3.3 Comparison of fitting goodness among the three distributions 40
Table 3.4 Whisker growth angle distribution 42
Table 3.5 Group-growth rate of mean length 43
Table 4.1 Geometry parameters of the SOPs 55
Table 4.2 Predicted distributions of the growth parameters 55
Table 4.3 Simulation procedure (I) 56
Table 4.4 Simulation procedure (II) 57
Table 4.5 Simulation risk with time 58
Table 4.6 Results of bridging number distribution 59
Table 4.7 Distributions of relevant parameters of free whiskers 66
Table 4.8 Simulated risk of the SOP with time 68
Table 5.1 Whisker growth measurement results of the non-coated sets 74
Table 5.2 Growth angle distribution 74
Table 5.3 Prediction of whisker growth and the corresponding bridging risk 75

List of Figures

Figure 1.1 Image of a kinked whisker 3
Figure 1.2 Atom diffusion and whisker growth for Sn plated over Cu 6
Figure 1.3 Average intermetallic thickness for tin, Sn-40Pb, and Sn-10Pb plating at 24 ºC and 50 ºC [20] 7
Figure 1.4 Whiskers grown along scratches on bright tin plated copper 8
Figure 2.1 Bridging failure caused by tin whiskers 20
Figure 2.2 Arcing failure caused by tin whiskers 21
Figure 2.3 Whiskers on the Armature 22
Figure 2.4 Contaminations on optics caused by whiskers 23
Figure 3.1 Distribution of whisker length in the 8th month storage in room ambient 38
Figure 3.2 Distribution of whisker length in the 13th month storage in room ambient 39
Figure 3.3 Distribution of whisker length in the 18th month storage in room ambient 4] 40
Figure 3.4 Probability density function curves of whisker length 41
Figure 4.1 Potential risk posed by conductive whiskers 46
Figure 4.2 Whisker bridging two adjacent conductors 48
Figure 4.3 Flowchart of fixed risk assessment (I) 50
Figure 4.4 Flowchart of fixed risk assessment (II) 53
Figure 4.5 Flowchart of fixed risk assessment (III) 54
Figure 4.6 Bridging simulation risk with time 58
Figure 4.7 Bridging short caused by free whiskers 60
Figure 4.8 Procedure of free risk assessment (I) 62
Figure 4.9 Procedure of free risk assessment (II) 64
Figure 4.10 Procedure of free risk assessment (III) 65
Figure 4.11 Arrangement of parts on the printed wiring board 66
Figure 5.1 Configuration of a experimental coupon 71
Figure 5.2 Configuration of an experimental set 72
Figure 5.3 Whisker growth with time 78
Figure 5.4 Conceptual configuration of experimental vehicle 80
Figure 5.5 Design for quantifying the characteristic parameters 81
Figure 5.6 Test design for contact resistance 82
Figure 7.1 Whisker deposition zones 89
Figure 7.2 Maximum distance a whisker can reach 90

Chapter 1 Introduction of Tin Whiskers

As a result of the global lead (Pb)-free movement, mainly driven by government legislations and market forces [29], pure tin (Sn) and high tin Pb-free alloys have been widely adopted as the materials of terminal finishes. Electronic part manufacturers who fail to meet this requirement may be excluded from not only European but also the other global markets. A major drawback of using lead-free tin finishes is tin whisker formation. This chapter provides the background of tin whiskers.

1.1 A Brief Description of Lead-free Movement

Electrical and electronic products and components are considered lead-free if they are assembled without the intentional use of lead in the raw materials or the manufacturing process [29]. JEDEC [35] defined "lead-free" devices as "solid-state devices that contain no more than 0.2% by weight of elemental lead". iNEMI [48] proposed a "lead-free" product as having "no lead intentionally added, and joints that have less than 0.2% lead by weight".

The basic goal of lead-free electronics is to eliminate lead from products and processes such that a known toxin can be kept from the waste stream. Various social and environmental elements have been contributed to push lead-free movement. Among those elements, government legislations and market forces [29] are the two main driving forces.

Current regulations regarding usage of lead in electronics are varied in scopes

and purposes [29]. Europe and Japan are the two pioneers in leading take-back legislation for various electronic and electrical products. The European Union (EU) has enacted legislations that would ban lead in electronics manufacturing from June 2006. In the United States, though there is no a legislation banning usage of lead, a change has occurred to catch the global lead-free movement.

With the growth of lead-free products, electronic parts manufacturers who fail to meet this movement may be excluded from not only European but also the other global markets. More and more electronics part providers have converted to lead-free products to replace lead-based products.

As a result of the lead-free movement, pure tin and high tin lead-free alloys are widely adopted by the electronics industry as a lead-free option, due mainly to their low cost, corrosion resistance and compatibility with lead-contained and lead-free solders. However, this change has prompted a reliability concern due to formation of conductive tin whiskers forming in pure tin and high tin Pb-free alloy finished surfaces.

1.2 Attributions of Tin Whiskers

A tin whisker is a tin crystal growing spontaneously from finished metal surfaces [6][7][16]. Whiskers are identified as long whiskers and short nodules. It should be noted that whiskers discussed in this dissertation are only needle-like whiskers but do not include nodules since nodules are short in length and pose much less risk than needle-like whiskers. Except tin, whiskers may grow in various types of metal surfaces, such as tin, zinc, cadmium, and antimony [59]. Metal whiskers usually

have some joint characteristics.

Whiskers can be straight, kinked, hooked or forked and lumpy [36]. Figure 1.1 illustrates the images of kinked and forked whisker, as an example. Solid, hollow, or perforated growth was also observed [56]. The outer surfaces of whiskers are often striated longitudinally.

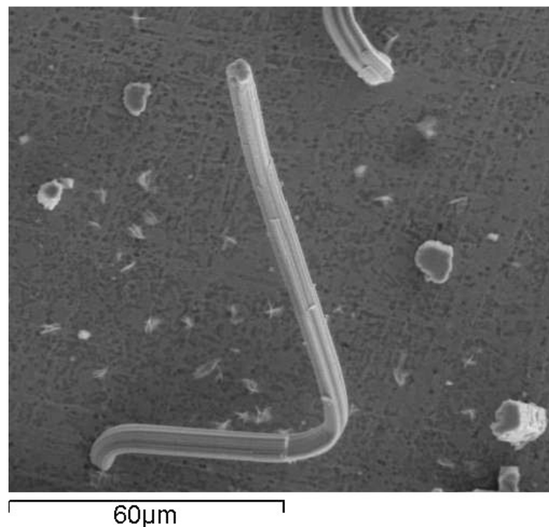

Figure 1.1 Image of a kinked whisker

Before intrusion from the metal finished surfaces, there exists an incubation period for whiskers. Experimental reports show that incubation period varies significantly days to years before whiskers appear [44], which may be associated with the change in compressive stress within the finish layer. This attribution is a concern because the observation period of the experiments designed to test the whiskering propensity for a particular process should be beyond the incubation periods in order to approach the reality. Variation in incubation period also make it difficult to predict whisker growth since it is impractical to calculate and estimate the incubation period.

Growth rate of tin whiskers can be up to 9 mm/year [8]. The rate of growth is not necessarily linear and a whisker may cease growth upon reaching certain length. Various factors, such as substrate materials, grain structure, plating chemistry, and plating thickness may influence growth rate.

Tin whisker length depends on growth rate and sustained periods of growth. Typically, fully developed whiskers are 500 μm in length and 0.3-10 μm in diameter. The longest whisker ever reported was 10mm [16].

Whisker density has been found to vary significantly for different application. The largest density ever reported is up to $10^4/cm^2$. But there exists variation in measuring whisker density. The variation is mainly caused by inconsistent definitions, such as the counting criteria and methods.

Typically current carrying capacity of a tin whisker is 10~32 mA, depending on the diameter of the whisker and the atmospheric environment [13]. The diameter affects the electrical resistance of a whisker and atmospheric environment determines heat removing from the whisker [7]. This is the reason that whiskers usually have a lower current capacity in vacuums and low-pressure conditions than in air.

A whisker is much significantly stronger in the axial direction than in the radial direction due to its crystal structure which makes the shear strength along the radial direction relatively low [18]. Whiskers can be broken under mechanical loading, such as vibration, shock and mechanical handling. However, experiments have demonstrated contradictory results. For example, Stupian's study [59] showed that whiskers could not be broken by mechanical shock or vibration because whiskers are

capable of withstanding elastic strains 100 times of bulk tin. However, no study has been conducted to measure whisker strength quantitatively.

1.3 Whisker Formation and Growth Mechanisms

Though study research on the issue of metal whiskers has been conducted for more than half a century, there is no a globally accepted model to describe whisker growth. Several models have been proposed for the mechanisms of whisker growth, such as dislocation model [21][41] and recrystallization model [1] [4][20]. Nevertheless, compressive stresses have been considered the driving forces for whisker formation and metal whiskering is identified as a form of energy release [37][66].

Dislocation model [21][41] states that a dislocation loop expands by climb. The dislocation loops glide to the surface of a whisker and deposit Sn atoms. Though the detail of the dislocation models proposed by different researchers were different, dislocation loops have been considered the driving vehicle to carry Sn atoms to grow whiskers.

Recrystallization-based model [1] [4][20] postulates that: (1) shear strain is introduced by plastic deformation and is stored in the metal in the form of dislocations (lattice defects); and (2) recrystallization can occur due to the low recrystallization temperature of tin. Whisker formation is considered as a nucleation and growth phenomenon, in which the energy released by whisker growth is greater than that required for creating additional surface area.

Various factors appear to contribute to compressive stress, including formation

of intermetallics (IMC) between the interface of plating and substrate, presence of residual stresses within substrate and plating, mechanical loading, surface damage, and mismatches in coefficient of thermal expansion (CTE) of plating and substrate or under-layer [38].

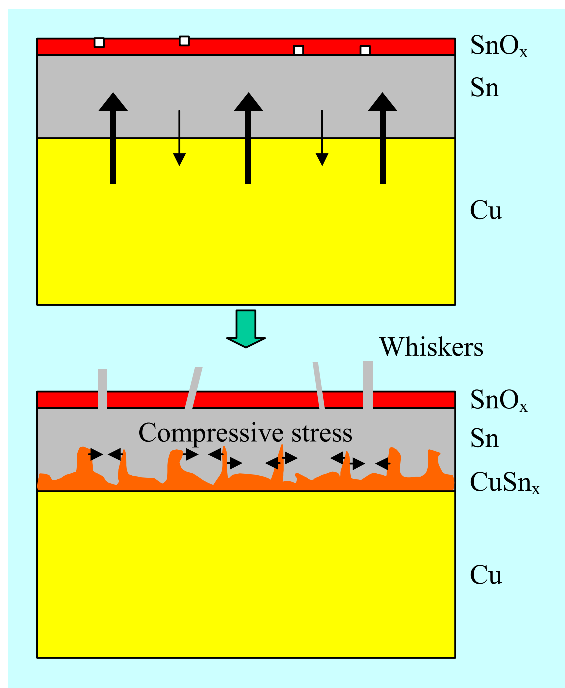

Figure 1.2 Atom diffusion and whisker growth for Sn plated over Cu [17]

Compressive stress can be generated by intermetallics formed in the interface of tin plating and the substrate materials [37], such as copper and brass. In the case of tin plated over copper leadframe, copper atoms diffuse into the adjacent the tin plating while very few tin atoms diffuse into the copper substrate, creating intermetallics of Cu_6Sn_5 and Cu_3Sn as illustrated in Figure 1.2. The densities of copper, tin and Cu_6Sn_5 are 8.96, 7.30 and 8.26g/cm^3, respectively. This causes slight reduction of the total

volume of the system after the IMC formation.

The IMC formation itself will not lead to compressive stresses in the tin deposit if the intermetallic compound layer forms flatly [37]. However, the diffusion is not distributed evenly throughout the interface of the coating and the substrate, and is dominated in the tin grain boundaries [65]. Consequently, the Cu_6Sn_5 layer is not flat and penetrates into tin grain boundaries; and thus results in compressive stresses. Figure 1.3 shows the average thickness of intermetallic compound between the plating and the substrate at 24ºC and 50ºC for both pure tin and two tin-lead plating compositions. Also IMC growth will alter the lattice spacing, compress the remaining tin layer, and apply tension on the substrate [17].

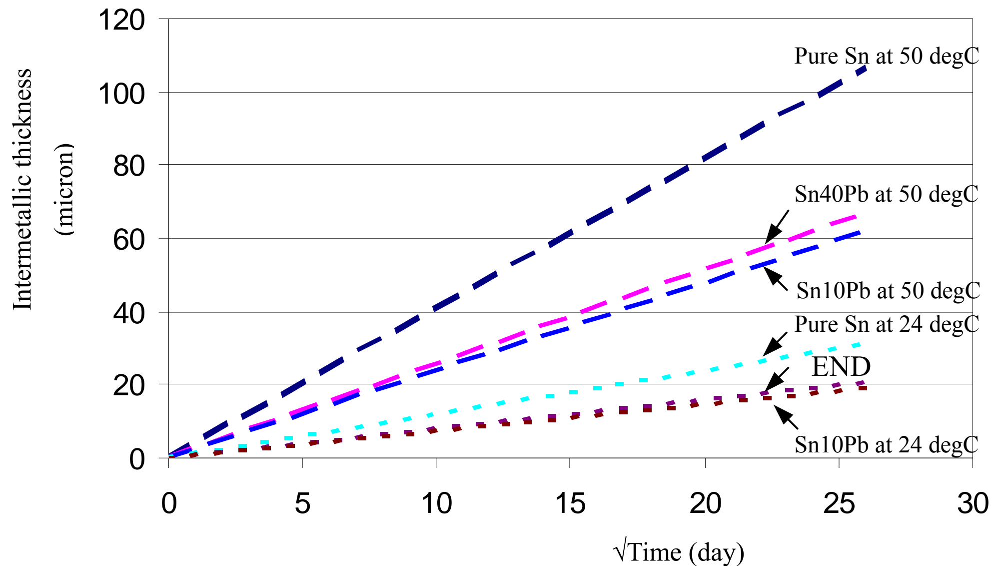

Figure 1.3 Average intermetallic thickness for tin, Sn-40Pb, and Sn-10Pb plating at 24 ºC and 50 ºC [20]

Compressive stresses caused by IMC increase with time since atom diffusion keeps continuing for. But tin oxide, formed in the tin surface, prevents the stress from

being released. Whiskers will grow, as a way of energy and stress release, when the compressive stress becomes high enough to break through the defects in the oxide layer.

The residual stresses are influenced by the parameters in the plating chemistry and process, such as impurities, grain size, plating thickness, and current density. Electro-deposited finishes are considered more susceptible for whiskering because higher current densities have been observed to produce higher residual stresses.

Mechanical loading, introduced by mechanical bending in lead formation process, or turning a nut or screw, can create localized stress. High compressive pressure from bolts or screws has been shown to produce whiskers in tin deposits [13]. Damages of the finish surface, such as scratches and nicks, can also create stress and may function as a nucleation point for whisker formation as showed in Figure 1.4.

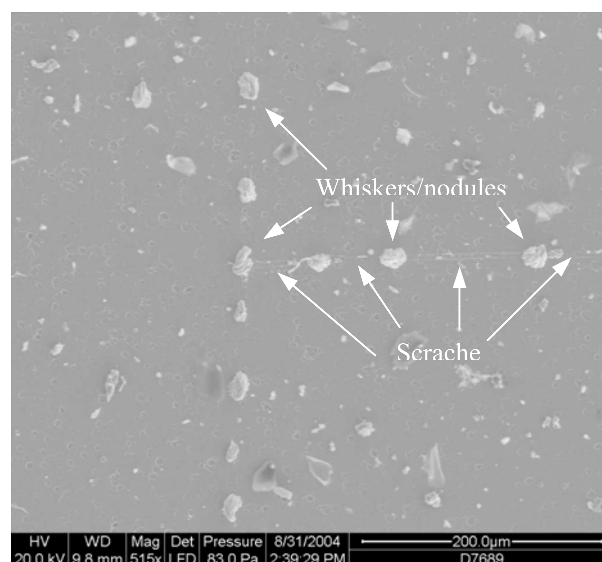

Figure 1.4 Whiskers grown along scratches on bright tin plated copper

Differences in coefficient of thermal expansion between the substrate or the

under-layer and the tin finish can cause stress at the interface. This is the reason that usage of Ni layer is effective in retarding whisker growth but cannot eliminate tin whiskering – Ni under-layer can significantly reduce formation of IMC, but cannot reduce mismatch of CTE among the different layers. There is a significant difference between the stresses caused by IMC and CTE – under isothermal conditions, IMC formation is the dominant source for generating internal stress; whereas under thermal cycling conditions, CTE is the dominant source [66].

Whisker growth is the result of the complex interaction among the various factors. Each factor discussed above may contribute to compressive stress formation. The dominant whiskering factor(s) varies for different applications, such as different plating processes, plating and substrate materials and environmental conditions.

1.4 Effects of Environmental Factors on Whisker Growth

It is still uncertain regarding the effects of environmental factors on whisker formation. The environmental factors include temperature, barometric pressure, humidity, thermal cycling and electric field. Experimental results have shown somewhat contradictory conclusions on the effects of environmental factors [42].

Elevated temperature increases diffusion and formation of intermetallics, but also relieve internal stresses. It appears that the optimal temperature for whisker growth is 50 ºC [8]. The temperature range that whiskers have been observed to grow is -40 to 150 ºC [8][43].

Barometric pressure appears to have little effect on whisker growth. Whiskers can grow in both atmospheric pressure and low pressure or vacuum conditions [8][43].

The fact that whiskers can develop in low pressure or vacuum conditions shows that oxidation is not a requirement for whiskering.

Experiments have demonstrated the contradictory results on the effect of humidity on whisker formation. For example, some experimental results showed increased whisker growth in high humidity (85~95 %RH) environment, but others showed no or little effect [8][43].

Similar to humidity, thermal cycling has shown contradictory effect on whisker growth in the experiments. Some experiments have shown high whisker growth rate in cycling -40 to 85 ºC [49], but others showed no any effect [7][8].

Whiskers can grow without applied electric field. However, electric field can create electrostatic attraction between whiskers and other conductors. This may increase the likelihood of whisker induced bridging shorts [67].

1.5 Mitigation Strategies

Though tin whiskers clearly present reliability problem, no accepted model and accelerated factors available to describe and predict whisker growth. Nevertheless, the electronics industry is currently facing the issue of how to retard whisker growth on the electronic products in a practical way. Various mitigation strategies thus have been proposed and applied by the electronic part manufacturers or customers to reduce tin whiskering. Below is a list of proposed mitigation strategies discussed in [45] and [50].

- Avoid pure tin plating
- Apply solder dipping

- Select matte or low-stress tin as the finish material
- Use underlayer
- Vary thickness of tin plating
- Avoid applying compressive loads on plated surfaces
- Apply heat treatments
- Apply conformal coating
- Strip and replate

The safest strategy to prevent tin whisker formation is to avoid using pure tin and high tin alloy as the plating material for any electronic components. Utilizations of procurement specifications with clear restrictions against the use of pure tin plating are highly recommended. For example, most of the commonly used military specifications currently have prohibitions against pure tin plating. Studies have shown that alloying tin with at least a second metal can reduce the propensity for whisker growth. However, experimental results have showed whisker growth from tin-lead alloys plated surfaces. Fortunately, the observed whiskers were much smaller than those from pure tin plated surfaces and may not pose a significant failure risk.

Solder dipping is an alternative mitigation strategy. However, solder dipping may cause damages to the components, such as package cracking or loss of hermeticity, due to thermal shock, popcorning of plastic packages, solder bridging between leads on fine pitch packages, and electrostatic discharge. Solder dipping may have limited success, depending on the specific process to coat the entire exposed tin plated lead surface. In order to reduce the potential risk from thermal shock to the

package, a stand-off distance to the package body is required in solder dipping. This stand-off area can be the portion where whiskers grow.

All types of pure tin finishes have the potential for whiskering. But bright electroplated tin finishes have been found to generate the highest density and longer whisker growth compared to matte tin finishes [6] and this is the reason that matte tin is recommended to be used instead of bright tin.

A thin layer of nickel over the copper substrate can significantly reduce diffusion of copper into pure tin finish. The benefit is that less IMC will form and less stress will be generated by IMC. However, Ni underlayer cannot eliminate whiskering due mainly to the fact that Ni underlayer cannot reduce the mismatch of CTE between the substrate or the underlayer and the tin finish [66].

Thickness of tin plating is also affect tin whisker growth. Glazunova [31] reported that whiskers did not grown on very thin (~0.5μm) tin plating while much higher whisker density and growth rate were found on thick (2~5μm) plating. Though very thin tin plating retards whisker growth, in reality very thin tin plating is not applied because tin plating with very thin thickness has poor corrosion resistance and solderability. Thick tin plating is required for real products. iNEMI recommended tin thickness for components without nickel or silver underlayer should be 10 μm nominal (at least 8 μm) or thicker in their interim recommendation [47].

Mechanical loading can create localized stress and thus cause whisker growth. Avoiding mechanical loading, such as mechanical bending, turning a nut or screw, is an effective way to reduce tin whiskering.

Heat treatments, including reflow, fusing and annealing, are promising method to prevent whisker growth. It is hypothesized that the high temperature involved in heat treatment relieves the internal stresses and increases grain size. It is recommended that heat treatment should be conducted in inert atmosphere and cooled slowly to avoid stresses reloading. Some experimental results show that heat treatment appears to reduce whisker density, but some demonstrate heat treatment is not an effective mitigation method [8] [32].

Conformal coats can suppress whisker growth, contain whiskers growing within the coat, and prevent whiskers from shorting exposed conductors. The effectiveness of a conformal coating depends partially on the coating material and the thickness of the coating. Conformal coating should be selected by considering various properties, such as CTE, modulus, adhesion strength, material toughness, and reworkability of coated assemblies to properly lessen the tin whisker risks. NASA Goddard experiments indicated that Uralane-5750 conformal coating can reduce whisker growth rate [39]. The results showed that a few whiskers penetrated through a 0.25 mil thick Uranlane-5750 coat after 2.5 years of room ambient storage; but no whiskers grew through the one mil thick coating until 3 years.

Stripping and replating are alternative methods to reduce whisker growth in the whisker prone areas. Pure tin plating is stripped and a suitable alternative plating, such as tin-lead or nickel is replated. Typically, leads on a package were replated with tin based alloys containing at least 3% of lead [44]. But the reliability of the original products can be negatively affected by the stripping and replate processes.

It should be noted that the strategies may not eliminate whisker growth completely; but can somehow decrease whisker growth, depending on the specific electronic parts and application. In addition, the trade off among reliability requirement, product and mitigation cost, and the controllability and effectiveness of the mitigation strategies, need to be considered.

1.6 History Research on Tin Whiskers

Metal whiskering phenomenon is not a new subject though selection of pure tin and high tin lead-free alloy as a terminal finish alternative has resulted in the renewed reliability concern regarding conductive tin whiskers formation. More than half a century ago, observations and research on whiskers were conducted due to various failures caused by cadmium whiskers. Following is a brief description of the milestone work in the tin whisker research history.

Metallic whiskers caught research interest after the cadmium whiskers were found to grow in the electroplated surface of the electronic components and caused bridging shorts. The first observation and research on cadmium whiskers was conducted by Cobb in 1946 [10].

A series of studies on metal whisker formation were initiated by Bell Laboratories in 1951 after cadmium whiskers were identified as the root cause of the failures of the channel filters [11]. It was found that whiskers grow not only on cadmium coating, but also on zinc and tin coating.

Tin whiskers became the research focus after tin and high tin alloys were used popularly as plating materials due to their low contact resistance, corrosion resistance,

and solderability. Several whisker growth models were proposed.

The first dislocation model for tin whisker growth was proposed by Peach [52] in 1952. Atom migration of tin through a screw dislocation at the center of the whisker was suggested by Peach as the reason of whisker growth. Peach concluded that the atoms were deposited at the tip of whiskers after the migration. However, testing results demonstrated that whiskers grew from the base but not from the tip.

Eshelby [21] and Frank [25] independently proposed the diffusion-limited model which suggested whiskers formed from the dislocations at the whisker base. The Eshelby's model suggested the Frank-Read dislocation sources were the reason for whisker formation. The Frank's model stated that the rotating edge dislocation pinned to a screw dislocation and stayed in the same plane after each revolution. A layer of the atoms was deposited to the whisker base for each revolution [25].

Compressive stresses were identified for the first time as the driving force for whisker growth by Fish, Darken and Carroll [26] at US Steel in 1954.

Another dislocation model was proposed by Franks [27] based on the data from tin on steel substrate in 1958. Franks suggested that dislocations induced by whisker were pinned due to the lattice faults and would function as a dislocation source under stresses. The pinned dislocations could move by gliding to grow whiskers. Franks' model met three propositions of Fisher's theory [26].

Mitigation strategies were first discussed by Arnold [1] at Bell Laboratorie. Arnold suggested that alloying tin plating with lead [2], fused and hot-dipped tin [3] were the effective mitigation strategies. Low ambient temperature and low relative

humidity were recommended to reduce tin whiskers. In addition, Arnold commented that electric and magnetic fields posed no acceleration effect on whisker formation.

Recrystallization was first explained as a model for whisker formation by Ellis, Gibbons and Treuting at Bell Laboratories in 1958 [20]. This proposal was inferred from the experimental data, but not based on direct metallurgical evidences. Glazunova and Kudryavtsev [31] also considered tin whisker growth a form of recrystallization of tin plating in 1963.

Bi-metallic films of copper-tin vacuum-deposited over fused quartz substrates were investigated by Tu [60] at University of California (LA) in 1973. Stress induced by the intermetallics of Cu_6Sn_5 was first considered a key factor of whisker formation.

A two-stage dislocation model for the tin, cadmium, and zinc whiskers was proposed by Lindborg [41] in 1976. Grain boundary and dislocation-pipe diffusion were considered a factor for the high whisker growth rate in the first stage, which was a dislocation loop-expansion stage based on dislocation climb and vacancy diffusion. In the second stage, dislocations were created by a source and glided toward the surface of the whisker, and deposited a layer of tin atoms at the whisker grain surface.

A new concept of whisker formation, cracked oxide theory, was proposed by Tu [61] in 1994. A weak point and/or a crack of oxide layer enabled a localized relief of internal stresses by whisker growth protruding through this weak point. Whisker growth rate was calculated based on various whisker characteristics, including stress level in the film, temperature, whisker spacing.

Direct measurement of residual stresses in tin plating was conducted by Lee

and Lee [37] at Seoul University in 1998. The major findings included: (1) initial stress for as-deposited plating was tensile (11MPa) but decreased to zero quickly, and thereafter increased to a compressive stress (-8MPa); (2) annealed samples; (immediately after deposition, at 150ºC) had zero stress and remained stable over time; (3) no significant increase in grain size after heat treatment was observed; and (4) the tin grains, from which whiskers grew, were always oriented differently from the major grain orientation in the coating.

Plating tin electroplated over copper with nickel underlyer was investigated by Xu [65] at Lucent in 2001. Compressive stresses was found to create over time for tin plated on copper substrates. Focused Ion Beam (FIB) analysis was first applied for tin whisker study. The results showed that the roots of whisker grains were connected to tin-copper intermetallics.

An Eyring accelerated model was used by Okada [49] to estimate lifetime cycle when a whisker reached 50 μm given the upper temperature was 85 °C in 2003. The experiments also showed that if the upper side temperature of thermal cycling was fixed at 85 °C, whisker growth was more accelerated when the lower side was lower.

An algorithm to assess tin whisker risk was proposed by Pinsky [53] [54] [55] at Raytheon in 2004. A whisker risk level 1-5 classification standard was proposed to correlate the potential risk to the mitigation for tin and zinc whisker issue. The algorithm was created to evaluate tin whisker risk to reflect the mitigating affects of conformal coat usage, along with a list of required application specific risk

assessment threshold values for each whisker mitigation level was provided.

The distinct from any previously reported whisker growth on either pure tin or other tin-based alloy electrodeposits was reported by Chen and Wilcox [9] at Institute of Polymer Technology and Materials Engineering, Loughborough University. The incubation period was only a few hours, followed by a spectacularly rapid and profuse growth. It was found that the tin-manganese electrodeposits were in a tensile residual stress state during the whole period of whisker growth. This was a challenge to the commonly accepted explanation that the driving force for tin whisker growth is compressive stress.

In summary, tin whisker research has achieved substantially in the past half a century though the growth mechanisms are still not well understood. Compressive stresses are widely considered the driving forces for whisker growth.

Chapter 2 Problem Statement, Dissertation Objectives and Scope

In this section, tin whisker risk and the field failures are briefly reviewed. The current efforts to evaluate the risk posed by tin whiskers are introduced and discussed. The motivation, the objective and scope of this work are presented.

2.1 Overview of the Risks Associated with Tin Whiskers

Whiskers can cause failures of electronic products. The potential risks posed by tin whiskers are identified into three categories – bridging short, metal vapor arcing and plasma, and debris or contamination [7][50]. Following discussions are based on the two references.

Conductive tin whiskers can create electrical shorts by bridging the adjacent conductors in two ways. The first way of bridging occurs if a whisker reaches to the adjacent conductors from the conductor on which it develops. Another way of bridging is related to broken free whiskers. The whole or a part of a whisker can break off from its original growth sites under external loading, such as mechanical handling and vibration. Broken whiskers can float with airflow since they are tiny and light, and may drop into other sites and bridge adjacent exposed conductors. Shorts caused by whiskers can be permanent or transient, depending on the current capacity of the whiskers and the applied current. A transient short may occur if the current exceeds the fusing current of the whisker. Otherwise, a permanent short occurs.

A catastrophic failure may occur if a whisker fuses open with a current of more than a few amps and a supply voltage over 12 volts in a vacuum or low-pressure

environment. The vaporized tin may initiate plasma, which can conduct over 200 amps of current and may continue until all the available exposed tin is consumed or the supply current is interrupted.

Broken whiskers can potentially be a source of debris and contamination. They may interfere with the smooth operation of micro-electro-mechanical structures (MEMS) or contaminate optical surfaces.

2.2 Field Failures Caused by Whiskers

Reports from the electronics industry have shown numerous electronic field failures associated with tin whiskers, which have resulted in millions of dollars loss [7][51]. Below are several case studies on field failures caused by tin whiskers.

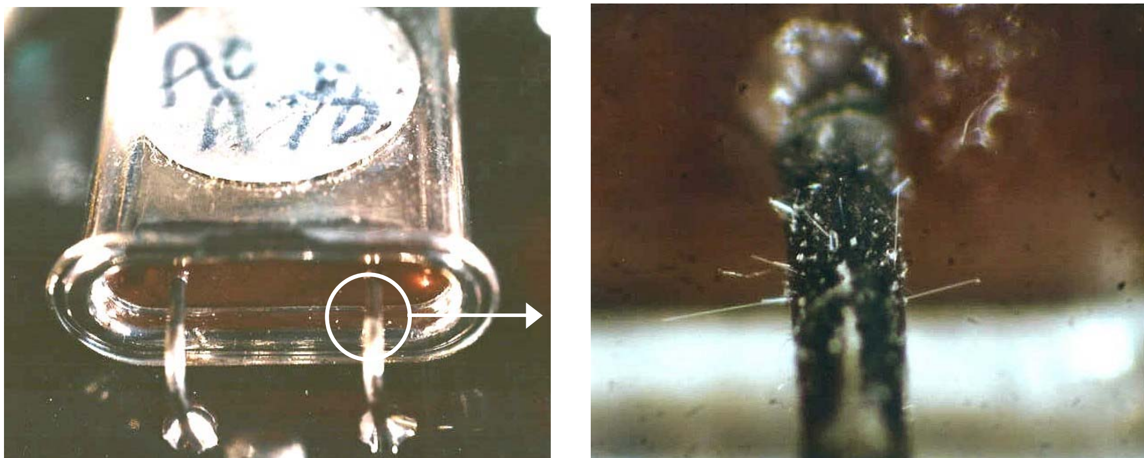

Figure 2.1 Bridging failure caused by tin whiskers [46] (Courtesy of the NASA Electronic Parts and Packaging Program)

The component shown in Figure 2.1 was a crystal oscillator package which had two lead-wires with bright tin finished over the nickel underlayer [46]. The two

lead-wires was exposed to tin-lead hot solder dipping within 1.27 mm to the package to improve solderability before being mounted on the printed wiring board (PWB). A loss of oscillator output was found approximately one year after the oscillator had been installed. Failure analysis demonstrated that tin whiskers had grown on the portion of the lead-wires which were not covered with tin-lead solder during the assembly process. The whisker, which bridged the lead wire and the case, was 1.5 mm in length. It can be seen that the uncovered portions from solder dipping are potential risk areas where tin whiskers can grow.

Figure 2.2 Arcing failure caused by tin whiskers [14] (Courtesy of G. Davy, Northrop Grumman Electronic Systems)

Figure 2.2 illustrates a failure of a type of relay used on the military airplanes for about fourteen years [14]. Through the hole in the case, one may observe a coating of soot on all surfaces, melted parts at the end of each terminal stud, and the edge of the iron armature, which was bright tin-plated. Possible root causes resulted in the failure of the relay, which initiated the current surge to the ground, could be wearout,

loose particles, or metal vapor arcing.

After several steps of failure analysis, it was concluded that it were the tin whiskers which initiated the current surge to the ground. Many whiskers were found, as illustrated in Figure 2.3, to grow on the armature and the longest one was 2.5 mm in length. But the spacing between the armatures and the terminal studs was 1.8mm. A self-sustaining arcing occurred when a whisker bridged between the terminal stud and the armature and melted open for this case [14].

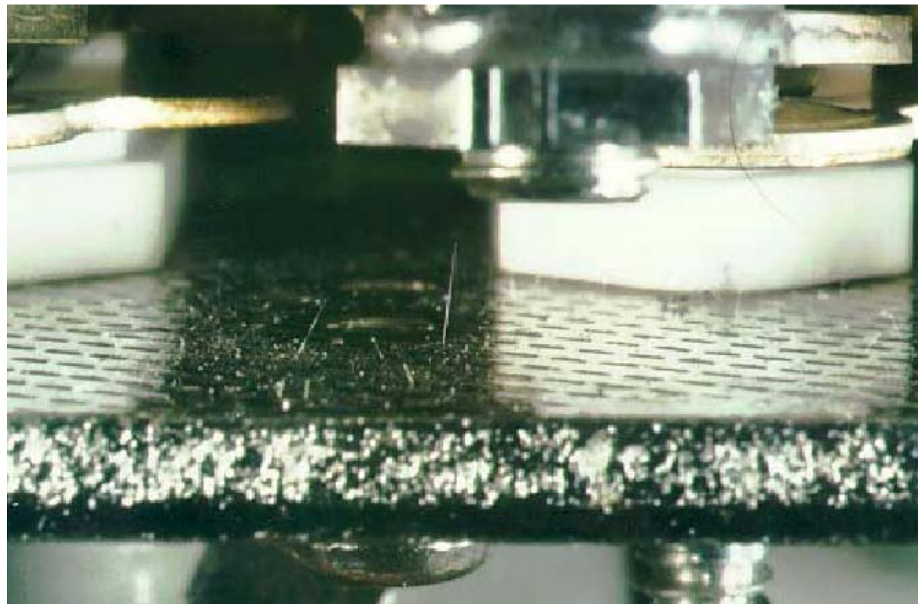

Figure 2.3 Whiskers on the Armature [14] (Courtesy of G. Davy, Northrop Grumman Electronic Systems)

Figure 2.4 shows a case that an optical instrument was interfered with a tin whisker. The whisker might be considered mistakenly a scratch on the sample. This could result in an incorrect analysis result.

Figure 2.4 Contaminations on optics caused by whiskers [46] (Courtesy of the NASA Electronic Parts and Packaging Program)

2.3 Previous Efforts to Quantify Bridging Risks Associated with Tin Whiskers

Previous approaches to assess tin whisker risk include the risk assessment algorithm developed by Pinsky [53][55] at Raytheon and the reliability approach model by Okada et al [49] at Murata Manufacturing Corporation, Ltd.

2.3.1 Pinsky's risk assessment algorithm [53]

Pinsky developed an algorithm to assess the bridging risk caused by tin whiskers between adjacent conductors. The bridging risk was defined as "overall mechanical risk" in Pinsky's paper, which was the product of the probability that whiskers grow and the probability of these whiskers bridging between conductors. The factors that affect whisker growth relate to the properties of the plating and the substrate onto which pure tin is plated, while the factors that affect the bridging risk relate to the geometry of the assembly and the presence or absence of insulating

coatings on the conductors.

The output of the algorithm was a numerical index of relative risk of whisker bridging and the numerical index was reported on a log-10 scale. Scaling factors have been selected so that the range of the numerical factor was between zero and 10. Higher output numbers indicated higher degrees of risk. The overall mechanical risk was expressed as:

$$R_{total} = K + \log_{10}(R_{geom} \cdot R_{growth}) \qquad (2.1)$$

where R_{total}, R_{geom}, R_{growth} and K were the overall mechanical risk, total geometric risk factor, overall whisker growth risk factor and scaling constant respectively.

For geometric risk factor, there were four independent driving mechanisms of concern, including 1) stress induced during initial tin deposition; 2) stress developed in the tin as a result of inter-diffusion with the material below during time/temperature exposure; 3) stress developed over time due to differential CTE between the tin and the controlling substrate; and 4) stress induced as a result of externally applied forces. Therefore, total geometric risk factor could be calculated by:

$$R_{growth} = R_i + R_d + R_{cte} + R_{ex} \qquad (2.2)$$

where R_i, R_d, R_{cte} and R_{ex} were initial stress risk factor, diffusion stress risk factor, CTE stress risk factor and external risk factor, respectively.

There were two ways for whiskers bridging adjacent conductors. The first way was by growing from one conductor and reaching across to a conductor adjacent to the tin-plated conductor, which was called “direct bridging”. The second one was for a whisker to from and then break off from its growth site, and then later form a bridge

between two other conductors elsewhere, which was called “secondary bridging”. Total geometric risk factor then could be expressed by:

$$R_{geom} = R_{gd} + R_{gs} \qquad (2.3)$$

where R_{gd} and R_{gs} geometric risk factor for bridging from site of whisker growth, geometric risk factor for dislodged whiskers.

By combining the above three equations, the overall mechanical risk could be described as:

$$R_{total} = K + \log_{10}[(R_{gd} + R_{gs}) \cdot (R_i + R_d + R_{cte} + R_{ex})] \qquad (2.4)$$

Each of the six R_x values in equation 2.4 was calculated based upon attributes of the application.

$R_{gp} = f\ \{r_1, r_8\}$

$R_{gs} = g\ \{r_{10}, r_{11}, r_{12}\}$

$R_i = h\ \{r_2, r_3, r_4, r_7\}$

$R_d = l\ \{r_2, r_5, r_7\}$

$R_{cte} = m\ \{r_2, r_6\}$

$R_{ex} = n\ \{r_2, r_9\}$

where *f*, *g*, *h*, *l*, *m* and *n* are functions which were simple products of applications. These functions could be redefined later if data indicates a different type of relationship applies. The meaning of the functions were shown as below:

$r_1 = f_1$(conductor spacing)

$r_2 = f_2$(Pb content in plating)

$r_3 = f_3$(Sn deposition process)

$r_4 = f_4$(Sn deposit thickness)

$r_5 = f_5$(composition of material directly beneath Sn deposit)

$r_6 = f_6$(substrate controlling the CTE imposed on Sn deposit)

$r_7 = f_7$(reflow of Sn deposit)

$r_8 = f_8$(type of conformal coating applied directly over Sn deposit)

$r_9 = f_9$(use of mechanical hardware that applies stress to the surface of the Sn deposit)

$r_{10} = f_{10}$(vulnerability of the assembly to contamination related failure, as indicated by imposed environmental controls during assembly)

$r_{11} = f_{11}$(use of conformal coating on conductors throughout assembly)

$r_{12} = f_{12}$(airflow within assembly)

The functions f_x were defined as shown in Table 2.1. The scale factor K was set to be 8.9. Based upon the maximum and minimum values produced by the functions defined below, the numerical output to ranged from zero to 10.

Table 2.1 Risk factors [53]

Conductor spacing (mil)	Criteria	< 10	10-50	50-100	100-500	>500
	Relative Risk	2	1	0.5	0.25	0
Pb content (wt%)	Criteria	<0.2	0.2-1	1.0-3.0	3.0-5.0	>5.0
	Relative Risk	1	0.2	0.1	0.05	0.01
Process	Criteria	Bright	Matte	Immersion	Hot dip	-
	Relative Risk	1	0.5	0.3	0.1	-
Tin thickness (micro-inch)	Criteria	<50	50-250	250-500	500-1000	>1000
	Relative Risk	0.7	1	0.7	0.3	0.1
Material directly beneath tin	Criteria	Brass/bronze	Copper	Ferrous	Nickel	-
	Relative Risk	1	0.7	0.5	0.1	-
Substrate controlling CTE	Criteria	Ceramic	Low expansion alloy	Copper	Ferrous	Aluminum
	Relative Risk	1	1	0.2	0.3	0.2
Plating reheated	Criteria	No	-	Annealed	-	Fused
	Relative Risk	1	-	0.3	-	0.2
Conformal coating	Criteria	None	Urethane >1mil	Silicone >1mil	Parylene	Other
	Relative Risk	1	0.01	0.1	0.05	0.2
Use of mechanical HWD	Criteria	-	Fasteners	-	None	-
	Relative Risk	-	1	-	0.1	-
Where was assembly performed	Criteria	Clean room	Special clean area	Typical factory	Field assembly	
	Relative Risk	1	0.5	0.2	0.1	

Use of CC on conductors in enclosure	Criteria	None	Some	Most	All	-
	Relative Risk	1	0.7	0.4	0.01	-
Forced fluid cooling of assembly	Forced air	None	-	-	-	-
	1	0.1	-	-	-	-

Table 2.2 Simulated values of risk factors and the results [53]

Example #	r_1	r_2	r_3	r_4	r_5	r_6	r_7	r_8	r_9	r_{10}	r_{11}	r_{12}	Result
1	0.1	0.001	0.1	1	0.7	0.2	1	1	1	0.1	1	0.1	5.24
2	0.1	1	0.1	1	0.7	0.2	1	1	1	0.1	1	0.1	8.24

For a given application, the values of the risk factors contribution to whiskring can be obtained. The failure risk posed by tin whiskers can be estimated by applying the equations described in the above paragraphs. Below are two examples from Pinsky's paper:

Example I: Copper wire hot dipped into tin-lead solder, attached using a screwed-down lug, with the nearest conductor 0.25″ away, no conformal coat on any conductors, assembly under normal factory conditions. No forced air cooling.

Example II: Copper wire plated with bright tin 250 micro-inches, attached using a screwed-down lug, with the nearest conductor 0.25″ away, no conformal coat on any conductors, assembly under normal factory conditions. No forced air cooling.

The corresponding values of risk factors and the results of risks of the two examples are presented in Table 2.2. It can be seen that the tin whisker risk of example II is larger than that of example I.

2.3.2 Okada's reliability approach model [49]

Whisker growth experiments were conducted in thermal cycling conditions by Okada et al, and thermal cycling –40~85 °C with cycling period of 30 minutes demonstrated the best condition to grow whiskers. The experiments also showed that if the upper side temperature of thermal cycling was fixed at 85 °C, whisker growth was more accelerated when the lower side was lower.

An Eyring accelerated model was used to estimate lifetime cycle when a

whisker reached 50 μm given the upper temperature was 85 °C. The Eyring model was expressed as

$$\ln(L) = C - \alpha * \ln(\Delta T) \qquad (2.5)$$

where L was the lifetime; C was a constant; α was the thermal cycling acceleration coefficient; and ΔT was the temperature difference with upper side at 85 °C. The values of C and α were determined to be 69.04 and 12.65.

As an example in Okada's paper, the lifetime was 3.66×10^5 (more than 100 years) if the temperature cycling was 0~85 °C. From the results of the model, it was concluded by Okada that whiskers in thermal cycling condition would not pose reliability problem within the lifetime of the electronic devices.

2.4 Motivation of this Research

Tin whiskers growth is a dynamic phenomenon, which defines that risk related to whiskers is also a function of time. But Pinsky's algorithm was independent of time. The numerical index, the final result of his algorithm, did not assign an actual risk and it was still a qualitative analysis. In Okada's study, the model was only developed for thermal cycling with the upper bound of 85 °C. Whiskers can growth without thermal cycling. This limited the application of his reliability assessment.

With pure tin and high tin alloys adopted by more and more electronic part manufacturers as the materials of finishes, tin whiskering issue has become a reliability concern. No industry agreed methods have been developed to assess tin whisker risk. However, the electronics industry needs a practical methodology to assess tin whisker risk. The algorithm developed in this work is to fulfill this demand.

2.5 Objectives of this Research

The overall objectives of the research are:

1. To provide a methodology to assess tin whisker bridging risk on the electronic products quantitatively;
2. To design the experiment to simulate tin whisker bridging failure caused by fixed and broken free whiskers;
3. To demonstrate the methods to collect needed information from the experiments

2.6 Scope of this Research

This dissertation study focuses on development of tin whisker bridging risk assessment algorithm and design of the simulation experiments. As the fundamental base of the algorithm, the research on whisker growth is also conducted.

2.7 Description of this Dissertation

The body structure of this dissertation is composed of:

Chapter 1 provides the background of tin whiskers, including attributions of tin whiskers, whisker growth mechanism study, effect of environmental factors on whisker growth, mitigation strategies, and history of tin whisker research.

Chapter 2 states the potential risks posed by tin whiskers and shows the field failures caused by whiskers. Previous efforts to assess tin whisker risk are briefly described and discussed, and the motivation of this dissertation is provided.

Chapter 3 presents the approach to quantify tin whisker growth in terms of

whisker density, length and growth angle. Probabilistic and statistical methods are applied to describe tin whisker growth.

The development of the risk assessment algorithm is presented in Chapter 4. Risk related parameters and failure criteria are discussed, and the risk assessment procedures are provided.

Design of the simulation experiments is discussed in Chapter 5. Bridging shorts introduced by fixed and free whiskers are simulated. Experimental vehicles and conditions are specified, and the experimental results and analyses are presented.

The conclusions and summaries of this work are given in Chapter 6. The contributions of this work and the recommendations for the future work are provided in Chapter 7.

Chapter 3 Whisker Growth Analysis

The studies on whisker growth are presented in this section. The statistical and probabilistic models are applied to describe the parameters of tin whisker growth. Whisker growth parameters include whisker density, length, maximum length, growth angle, and growth rate. Whisker growth analysis serves as the fundamental information for the bridging failure risk from fixed whiskers.

3.1 Electronics Industry's Acceptance Level for Whisker Growth

In order to limit the risks posed by tin whiskers to electronic products, some electronic companies proposed acceptance level. For instance, the European semiconductor collaboration E4, formed by Philips, Infineon, STMicroelectronics and Freescale Semiconductor, was the first manufacturers to develop whisker acceptance levels with recommended test conditions [15]. Length of 50 μm has been chosen as the maximum whisker length at the device end of life by E4. iNEMI [58] tried to create a standardized whisker growth limit and proposed the maximum allowable whisker lengths for three classes of products, as shown in Table 3.1. Class 1 is assigned to mission and life critical high-reliability applications, such as military, space and medical applications. Class 2 is for high-reliability business applications, such as telecom infrastructure equipment and high-end servers, etc. Class 3 is suitable for consumer products with relatively short product lifetimes (typically within five years).

Table 3.1 iNEMI's whisker length limits [58]

Maximum Whisker Length			
Device (package type, lead pitch or operating frequency)	Class 1	Class 2	Class 3
Discrete device (2 pins)	Pure tin and high tin content alloys not acceptable	40 µm	67 µm
Multi-lead packages			(Minimum gap between leads ~ 0.05mm)/3 or 67 µm, whichever is smaller
Operaing frequency >6 GHz (RF) or $t_{rise}<59$ psec (digital)			50 µm

However, the acceptance level may not reflect the real risks posed by tin whiskers since only one parameter, whisker length, is used as the criterion. Other parameters, such as whisker density and growth angle, also contribute to tin whisker risk. In addition, the acceptance level is a qualitative analysis since it cannot evaluate tin whisker risk quantitatively.

3.2 General Description of the Experimental Study

In this study, tin whisker growth is expressed in terms of whisker density, length, maximum length, whisker growth angle and growth rate since these parameters determine the risk posed by tin whiskers for a specific application. Whisker density is the count over a fixed area, such as the number of whiskers per square centimeter. Whisker length refers to the length of a whisker beyond the plating surface from which a whisker grows. Maximum whisker length is the length of the longest whisker growing in the objective tin finished surfaces. Whisker growth angle is the angle of a whisker and its orthotropic projection against the finished surface

[37]. Growth rate describes time-dependent length of a whisker and time-dependent whisker density.

The measurement was conducted for the 72 coupons. The size of the coupons was 1″×1″×0.063″ in length, width and thickness. The thickness of pure tin plating over the substrate was 5 μm. Bright and matte tin were used as the finishing materials, and copper, brass (type 260) and alloy42 the substrate materials. The heat-treatments included Sn-Pb reflow profile, Sn-Ag-Cu reflow profile, temperature cycling (TC) between -40 and 80°C with 20 minutes dwell for 336 cycles, annealing (one week after plating) at 150 °C for two hours followed by temperature/humidity (T/H) at 60°C/95%RH for two weeks. After the exposures, all the coupons were stored in room ambient.

The measurement results can vary, depending on how it is conducted. The counting procedure we applied for density calculation was 1) environmental scanning electron microscope (E-SEM) was the tool to observe whiskers; 2) whiskers greater than 10 μm in length were counted; 3) 30 sites were randomly selected to take pictures by E-SEM and average whisker density was calculated based on the whiskers on these 30 sites for each coupon.

A microscope is needed for observing tin whiskers since they are usually very small. An optical microscope is not capable to observe whiskers because its magnification is limited and cannot distinguish whiskers from dusts. A SEM has high magnification and can take very clear pictures for the observed sites. The threshold was set to be 10 μm because whiskers, whose length is smaller than 10 μm, should

not cause serious reliability risks and can be excluded. Considering the length limits proposed by E3 and iNEMI as described previously, length of 10 μm is smaller than their limits and should be more conservative.

3.3 Whisker Density

The average whisker density can be calculated after the local density, which is the ration of whisker number and the observed site area, of the 30 sites are obtained. Normal distribution is considered the proper distribution to quantify whiskers, based on the central limit theorem (CLT).

The CLT [40] states that given a distribution with a mean μ and a variance σ^2, the sampling distribution of the mean approaches a normal distribution with a mean (μ) and a variance (σ^2/N) as N, the sample size, increases. The counter-intuitive thing about the central limit theorem is that no matter what the shape of the original distribution, the sampling distribution of the mean approaches a normal distribution [34]. For this case, there exists a real whisker density for a coupon or an electronic part as a point value. This density can be considered a delta function with the mean of itself. The measurement of the density is an approach to he mean. Therefore, whisker density in our measurement follows normal distribution.

Table 3.2 Results of the three measurements on whisker density [24]

Measurement time	8-month storage	13-month storage	18-month storage
Average density (#/cm^2)	14240	14390	14520
Standard deviation	5490	4820	3180
Density increasing rate (%)	-	1.1	0.8

Based on the experimental results, it was found that the coupon of bright tin plated over brass with exposures of annealing followed by T/H had the largest density among all the heat-treated coupons. The following whisker growth study, as a case study, was conducted on the coupons of bright tin plated over brass. Three measurements on whisker density were conducted in the 8th, 13th and 18th month storage in room ambient. The results of the measurements are presented in Table 3.2.

Whisker density during the periods of the three measurements only had a slight increase with the growth rates of 1.1% and 0.8% respectively. It appears that the density was converging and approaching the saturation point where whisker density will stop growing.

3.4 Whisker Length

Maximum length is often used to describe whiskering propensity and considered a tin whisker risk criterion. The longest whisker ever reported was 10 mm [16]. The longest whiskers may not reflect the comprehensive whiskering status and the potential risk even though maximum length is a key parameter. It may result in large uncertainty or even false conclusion if the maximum length is the only one parameter to evaluate whiskering propensity and the corresponding risk.

Whisker length is quantified by distribution instead of the maximum length in this study. Statistical distribution is a good method since whisker length varies among whiskers due to different incubation period and different growth rate. Distribution can also reflect the range and the trend of whisker length.

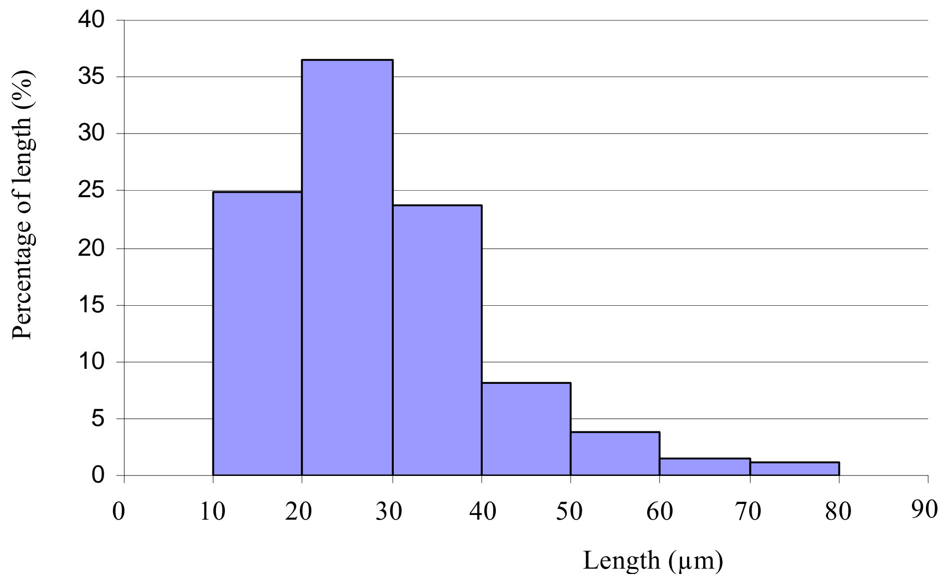

Figure 3.1 Distribution of whisker length in the 8th month

storage in room ambient [24]

Figure 3.1 shows the whiskers length bar distribution for the coupon of bright tin plated over brass in the 8th month storage in room ambient. It can be seen that whisker length in the range of 20 to 30 occupied the largest percentage, followed by the range of 10 to 20 μm and the range of 30 to 40 μm respectively. The collected data were fitted into a lognormal distribution. The mean was 24.0 μm and the standard deviation was 12.7μm.

Figure 3.2 illustrates the whisker length distribution in the 13th month storage in room ambient. Whiskers, whose length ranged from 10 to 40 μm, still dominated the percentage. Compared to the first measurement, the percentage of whiskers ranging from 10 to 20 μm decreased, while whiskers with the range of 10 and 20 μm increased in percentage and became the second largest group for this time. This phenomenon indicated that whiskers, as a whole group, continued to grow in length

during the four-month storage in room ambient. Lognormal distribution was still used to fit the data. The mean and standard deviation were 25.7 m and 11.5μm respectively, which were different from the previous ones.

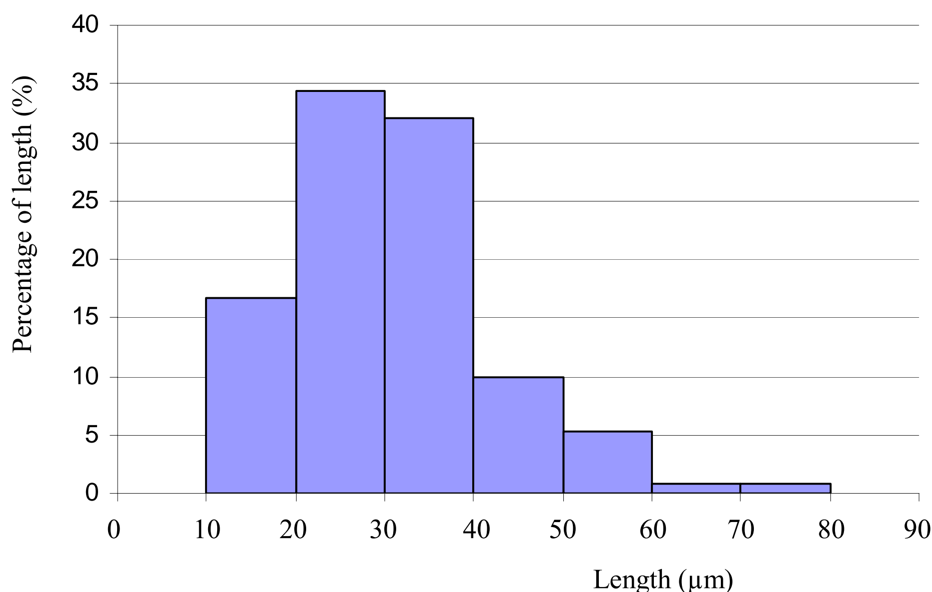

Figure 3.2 Distribution of whisker length in the 13th month storage in room ambient [24]

The whisker length distribution in the 18th month storage in room ambient is shown in Figure 3.3. The three largest percentage occupants were the same ones as in the 13th month. There were an apparent decrease in percentage for whiskers in the range of 30 and 40 μm and an apparent percentage increase for whiskers ranging from 30 to 40 μm. The change of the distribution still suggested that whiskers grew in length in the past five months. The mean and standard deviation were 26.0μm and 11.4μm respectively after the data were fitted into lognormal distribution.

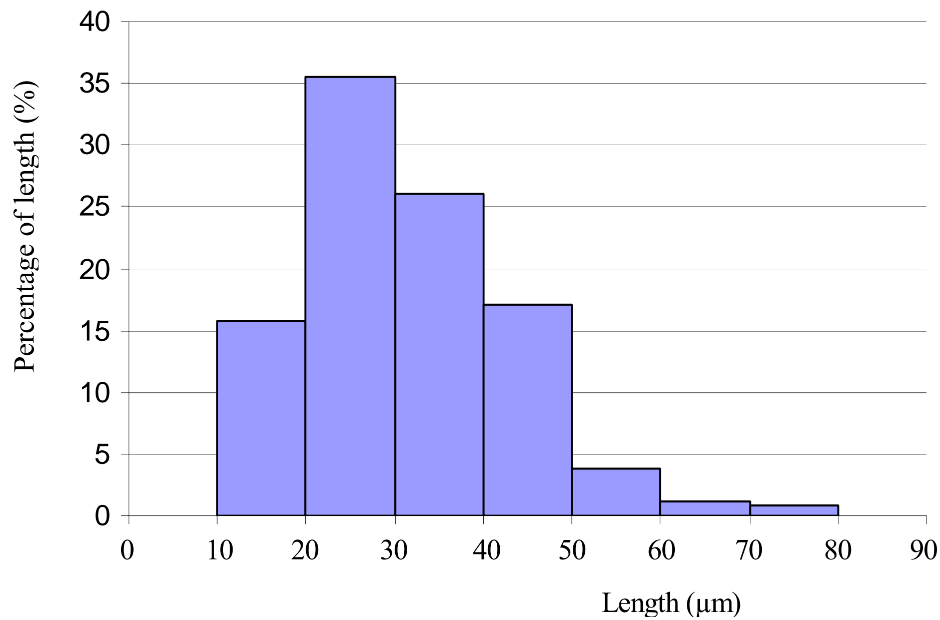

Figure 3.3 Distribution of whisker length in the 18th month storage in room ambient [24]

It is important to select a suitable distribution for whisker length. Lognormal distribution was selected to fit whisker length because it offers the best fit compared to other distributions. As shown in Table 3.3, lognormal distribution demonstrates better fitting goodness than others distributions for the measurements.

Table 3.3 Comparison of fitting goodness among the three distributions

Storage duration (month)		8	13	18
Fitting goodness	Lognormal	0.9997	0.9978	0.9967
	Weibull	0.9917	0.9925	0.9942
	Normal	0.9784	0.9821	0.9852

The probability density functions of whisker length for the three measurements are illustrated in Figure 3.4. It can be seen that the curves moved forward to right with time. This indicates that the group-whisker-length increases with time. The Figure also

shows that the distance between the neighboring curves is decreasing with time, which means growth rate of group-whisker length was approaching the saturation point. This phenomenon correlated to whisker density growth. It appears density and group-length may reach the saturation point at the same time.

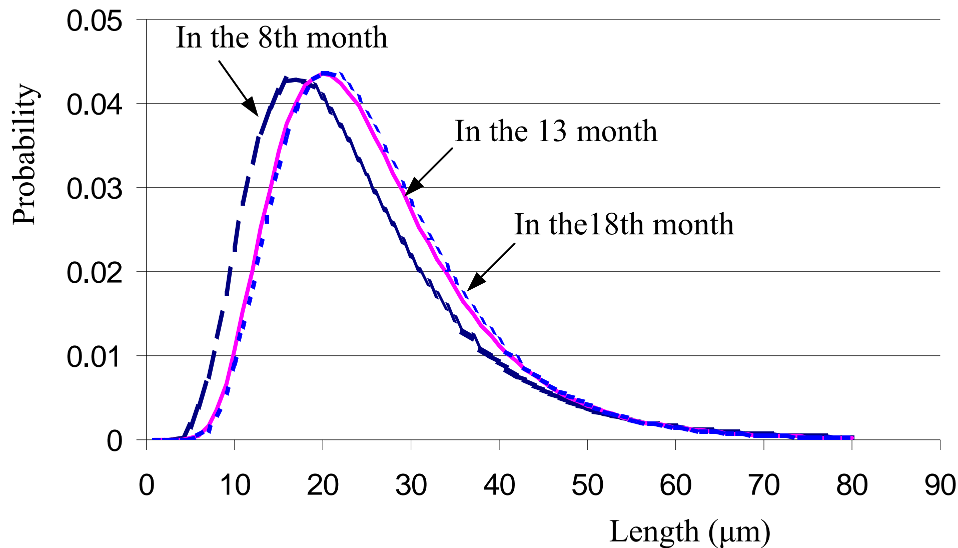

Figure 3.4 Probability density function curves of whisker length [24]

3.5 Whisker Growth Angle

No much attention and work has been paid to whisker growth angle in the previous studies; and growth angle appears to be ignored in the criteria of the electronics industry's acceptance levels. But growth angle is also a key parameter to affect tin whisker bridging risk. A whisker will not cause a bridging short if its growth angle is not large enough given that its length is greater than the spacing between the adjacent conductors. It can be over conservative without considering growth angle.

Table 3.4 Whisker growth angle distribution

Angle range (°)		0~10	10~20	20~30	30~40	40~50	50~60	60~70	70~80	80~90
Percentage (%)	8 -month	2.4	4.4	6.0	7.2	11.6	14.9	17.3	19.7	16.5
	13 -month	2.0	4.8	7.1	7.5	11.9	13.8	17.4	19.8	15.8
	18 -month	2.8	4.3	7.9	6.7	11.4	13.0	18.1	20.5	15.4

Growth angle of tin whiskers is distributed preferentially. Table 3.4 presents the range percentage of growth angle for the same specimen of bright Sn over brass. It can be seen that largest range of angle is between 60 to 90 degrees. This range dominates the largest percentage and angle range from 0 to 30 degrees is less common. The data with time also shows that whisker growth angle appear independent of time since the percentage of the ranges varied insignificantly with time.

Based on the data, the growth angle distribution is fitted as step-wise uniform; and uniformly distributed in four ranges of 0 to 20, 20 to 40, 40 to 60, and 60 to 90 degrees with the probability of 0.071, 0.146, 0.244, 0.539. The probability density function (PDF) of whisker growth angle in the 18-month can be express as:

$$f(\alpha)=\begin{cases}0.0035 & 0\le\alpha<20\\ 0.0072 & 20\le\alpha<40\\ 0.0122 & 40\le\alpha<60\\ 0.0180 & 60\le\alpha\le 90\end{cases} \qquad (3.1)$$

where α is growth angle in degrees.

3.6 Whisker Growth Rate

Individual whisker length is determined by the length growth rate. Several models on length growth rate have been suggested, such as Furuta and Hamamura’s model [28] and Tu’s localized model [61]. Furuta and Hamamura modeled whisker

growth rate as a function of vacancy formation energy, independent on tin-plating thickness. However, both the sample preparation process and the alloy utilized in the test were different from the industry techniques and processes which was the reason that this model was not adopted. Tu proposed a model, whereby the weak or cracked spots in the Sn oxide layer were considered as the dominant element for growth rate. Whisker growth rate was strongly affected by IMC, but no direct evidences were found to support this model.

Table 3.5 Group-growth rate of mean length [24]

Storage duration (month)	8	13	18
Mean length(μm)	24.0	25.7	126.0
Standard deviation (μm)	12.7	11.5	11.4
Maximum length (μm)	98	132	147
Average growth rate of mean length (μm/month)	3.00	0.34	0.06

Observations have shown that individual whisker length growth rate varies up to 9 mm/year [8]. However, range of individual whisker growth rate does not demonstrate group-whisker growth rate since, in this study, tin whisker bridging risk is considered the result of a group of whisker but not several whiskers though each individual whisker contributes to the risk. Whisker group-growth rate, such as group-growth rate of mean length, is the interest of this study. As presented in Table 3.5, the mean length group-growth rates were decreasing. The group-growth rate can be used to predict mean length of the whiskers using the rate at 18-month. This is a conservative estimation since growth rate is decreasing.

From Table 3.2 and Table 3.5, it appears that group-whisker-length growth

rate and density increase rate correlate to each other with the similar trend. The group-whisker-length growth rate increased when whisker density was converging.

3.7 Summaries of Whisker Growth

It is impractical to trace each individual whiskers to study their property and contributions to bridging failure since each individual whisker has its own length, growth rate and incubation period. Tin whisker related risks are the result of a group of whisker because, as a population, their growth and bridging behavior is dominated by the group-whiskers but not by several individual whiskers. Statistical distribution is a practical method to describe this group-whisker growth.

Though the study was mainly focused on the case of tin plated over brass in this study, the analytic methods and procedures are generic and can be applied for tin whisker growth in various application conditions. Whisker growth is one of the fundamental studies for tin whisker risk assessment.

Chapter 4 Development of Tin Whisker Assessment Algorithm

Conductive whiskers can cause bridging failure to the electronic and electrical products. How to assess tin whisker risk quantitatively has become a topic of the electronics industry. In this chapter, a tin whisker bridging risk assessment algorithm is developed. The goal of the algorithm is to provide the electronics industry a practical methodology to assess tin whisker risk quantitatively.

4.1 Fundamental Elements of the Risks Assessment Algorithm

Several elements, including risk categorization, risk parameters, and distribution of risk parameters, are defined as the bases to develop the risk assessment algorithm. Risk categorization identifies the sources of tin whiskers. Risk parameters are those parameters which directly contribute to or affect tin whisker bridging risk. Distribution of risk parameters discuss the best distributional models to the risk parameters.

4.1.1 Risk categorization

The bridging risk introduced by tin whiskers to an electronic product, such as a capacitor, a package, a board, or a computer system, can be identified as fixed risk and free risk as depicted in Figure 4.1.

The fixed bridging risk refers to an unintended electrical connection occurring due to the presence of a whisker growing from one or both surfaces, while the free bridging risk refers to an unintended electrical connection between two adjacent conductors occurring due to the presence of a conductive whisker which broke off

from its original growth site.

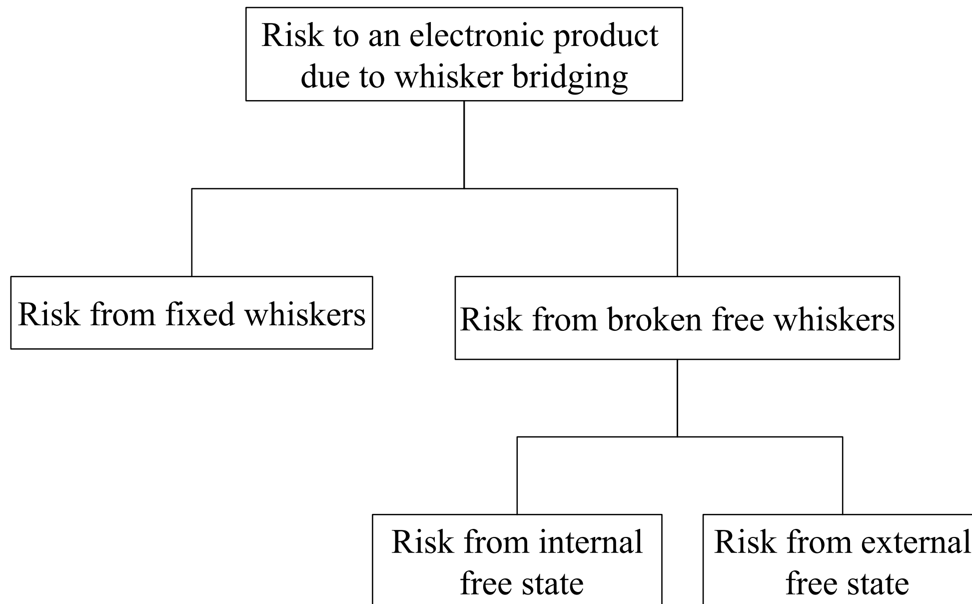

Figure 4.1 Potential risk posed by conductive whiskers

The free bridging risk can be further divided into internal free bridging risk and external free bridging risk. An electronic product is considered a control volume in this study. Internal free bridging risk is posed by the broken free whiskers formed inside the control volume, while external free bridging risk is induced by the broken free whiskers from the outside of the control volume.

4.1.2 Risk parameters

Risk parameters are those parameters that influence tin whisker risk directly. Fixed bridging risk and free bridging risk have the different parameters. Fixed risk parameters include whisker growth parameters and geometry parameters; while free risk parameters include whisker characteristic parameters and geometry parameters.

The whisker growth parameters are associated with the property of the integrated whiskers, including whisker density, whisker length, growth angle and growth arate. The characteristic parameters are associated with the property and performance of broken free whiskers, including broken free whisker density, broken free whisker length, deposition angle and probability of depositing on exposed conductors.

The geometry parameters describe the potential bridging sites in tin electronic product, including conductors where at least on structure has a pure tin or high tin finished conductor, and the amount of conductor area from which whiskers may grow in a product.

As a type of risk parameters, geometry parameters play an important role on tin whisker bridging risk. As a reference, the spacing between adjacent conductors for ultra fine-pitch, common fine-pitch, and typical surface-mount passive components are 50~100, 100~500 and 1000 μm, respectively [30]. As a result, ultra fine-pitch components have highest bridging risk given the identical applications. The impact of spacing on the bridging risk will be demonstrated in the section of risk assessment implementation.

4.1.3 Distributions of whisker growth parameters and characteristic parameters

Distributions are applied to describe the whisker growth parameters and characteristic parameters in this study. The distributions of growth parameters have been discussed in Chapter 3. Similar to the growth parameters, the characteristic parameters are also quantified in terms of distributions.

4.2 Risk Assessment for Fixed Whiskers

In this section, a bridging risk assessment algorithm for fixed whiskers is developed. The bridging risk is quantified by probability of failure due to a conductive whisker bridging the adjacent electrically isolated conductors and thereby producing an unintended electrical short at a particular time. The risk assessment algorithm is based on relevant inputs, bridging failure criterion, and is implemented a computer program.

4.2.1 Failure definition [23]

As a conservative approach, a bridging short is assumed to occur if

$$l_w \cdot Sin(\theta) \geq l_s \qquad (4.1)$$

This situation is illustrated in Figure 4.2 for a pair of parallel surfaces, where θ is the whisker growth angle; l_w is the length of the whisker; and l_s is the pitch spacing between the two adjacent conductors. This definition can also be applied to any shape of surfaces. Assume there are two adjacent non-lead conductors. To be conservative, the spacing can be considered the shortest distance between the two conductors.

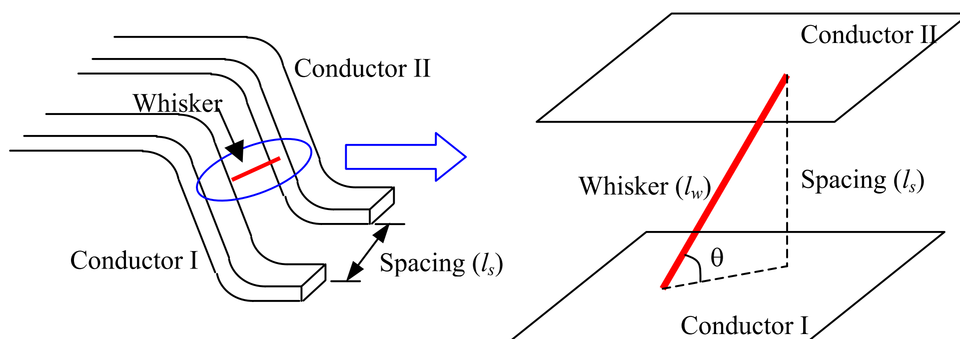

Figure 4.2 Whisker bridging two adjacent conductors

If only straight whiskers are considered, only surfaces facing each other can be at risk due to whisker growth. However, kinked whiskers have been observed. As a conservative assumption, the whole surface area will be considered to contribute to number of bridging opportunities. Another conservative assumption is that bridging spans shortest distance between conductors.

The conductor area depends on the shape. Assume a pair of conductors: tin plated square pad and a Cu cylinder. The conductor area can be considered the surface of the pad and the spacing is the short distance between the pad and the cylinder.

4.2.2 Whisker growth parameters and their distributions

The growth parameters of fixed whiskers include whisker density, length, and growth angle. The parameters and their distributions of the three parameters have already been discussed in Chapter 3.

4.2.3 Procedure to quantify fixed bridging risk in terms of probability

The fixed risk assessment procedure consists of inputs, simulation calculation and output. The inputs to algorithm include the whisker growth parameters, the geometry parameters, and the initial variables and control variables. The initial variables include number of failures which is set as zero initially, and the sample size of Monte Carlo simulation which also serves as control variable. Another control variable is the number of sampled whiskers. The output is the bridging failure risk for the specific conductors at a specific time.

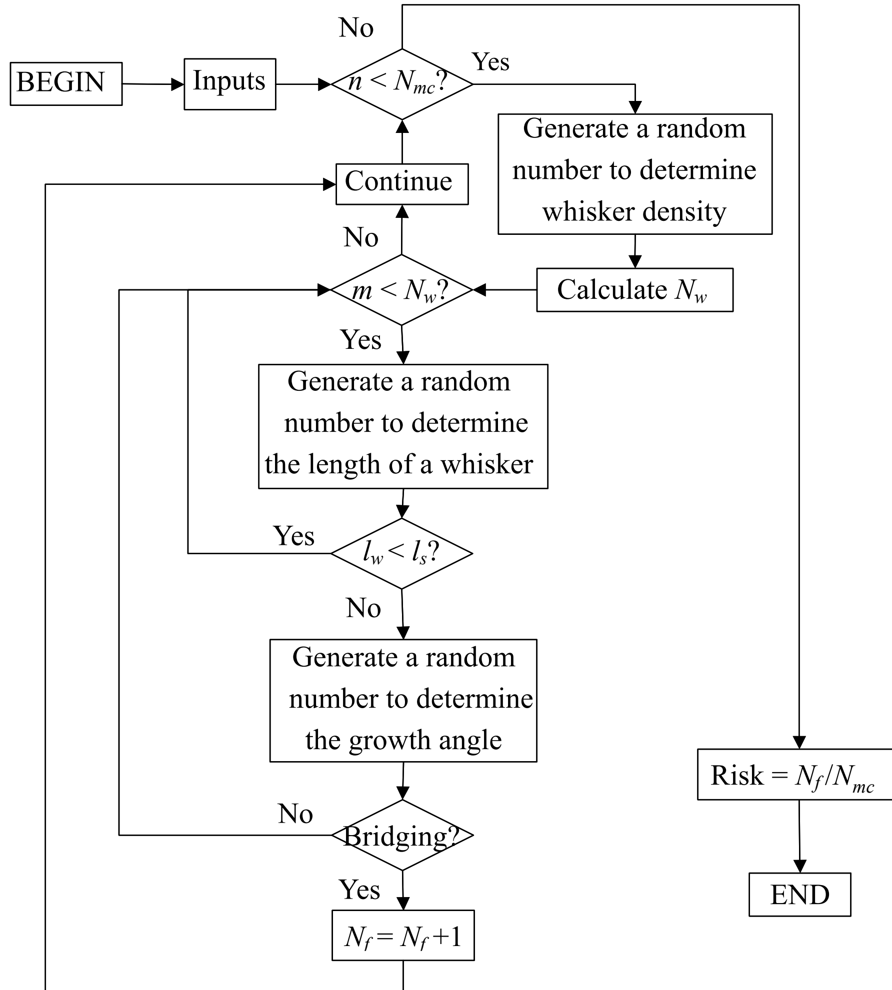

Figure 4.3 Flowchart of fixed risk assessment (I) [23]

Bridging failure risk at a particular time posed by tin whiskers is defined as the number of failures per number of potential failure opportunities (sample size of Monte Carlo simulation). The final risk of the objective conductors at a particular time by the Monte Carlo simulation is:

$$Risk = N_f / N_{mc} \tag{4.2}$$

The flowchart of the risk assessment procedure is presented in Figure 4.3, in which three random variables are generated to simulate a whisker density, length of a simulated whisker, and the growth angle of the simulated whisker. Generating a

random number means to order the computer to generate a random number between 0 and 1; and then to calculate the corresponding value using the inversed distribution function.

In the procedure, N_f, N_{mc}, l_w, l_{min}, and N_w represent the number of failures, the sample number of Monte Carlo simulation, length of a sampled whisker, the spacing of adjacent conductors, and the number of sampled whiskers in a simulation respectively; while n and m are the iteration control numbers of Monte Carlo simulation and simulated whiskers. N_f, the number of failures, will increase one if a failure occurs in a simulation.

The sample size of Monte Carlo simulation is determined by testing different numbers until the final answer of risk converges. The number of whiskers in a simulation is the product of sampled whisker density and the objective conductor area. Sample size of Monte Carlo simulation represents the number of the simulated electronic products. For example, if the sample size is 2500 and the simulation object is a hard drive, this means 2500 hard drives will be sampled and the risk is the ratio of the number of the failed hard drives and 2500. For each hard drive, whisker density, length and growth angle will be sampled according to the distributions.

The simulation will go to the next simulation if a first failure occurs. It is assumed that the product will fail immediately once the first bridging occurs, so it is not necessary to examine the other whiskers in the simulation since the product has already failed.

It should be noted that the procedure shown in Figure 4.3 is for a Monte Carlo

simulation at a particular time (usually, the design or mission life). If multiple times required, whisker growth data can be input into the algorithm as arrays; or the growth rates of mean of length and density be input such that mean of length and density can be calculated at each desired time.

In the procedure, whisker density, length and growth angle are assumed independent. The proof of this assumption will be shown in Chapter 5, section 5.1.2.

4.2.4 Procedure to quantify risk in terms of bridging number

In the above procedure, the risk of bridging failure is quantified in terms of probability of failure. This analysis is reasonable for the electronic products in field usage. It would be more meaningful if the bridging failure risk were quantified in terms of bridging number for the products in stock or stand-by state. Those products may lose function when they are applied voltage bias if their conductors are bridged by tin whiskers. The likelihood of failure of a product with larger number of bridging should be higher than the one with less number of bridging when the product is applied electrical current.

The procedure to quantify tin whisker bridging risk in terms of bridging number is shown in Figure 4.4. The inputs and the variables have the same meaning as the previous ones shown in Figure 4.3. But the density is a nominal value. Whisker length and growth angle will be sampled in the procedure. The output N_{fn} is the nominal bridging number. In this procedure, the nominal number of fixed whiskers is used to obtain the nominal number of failures.

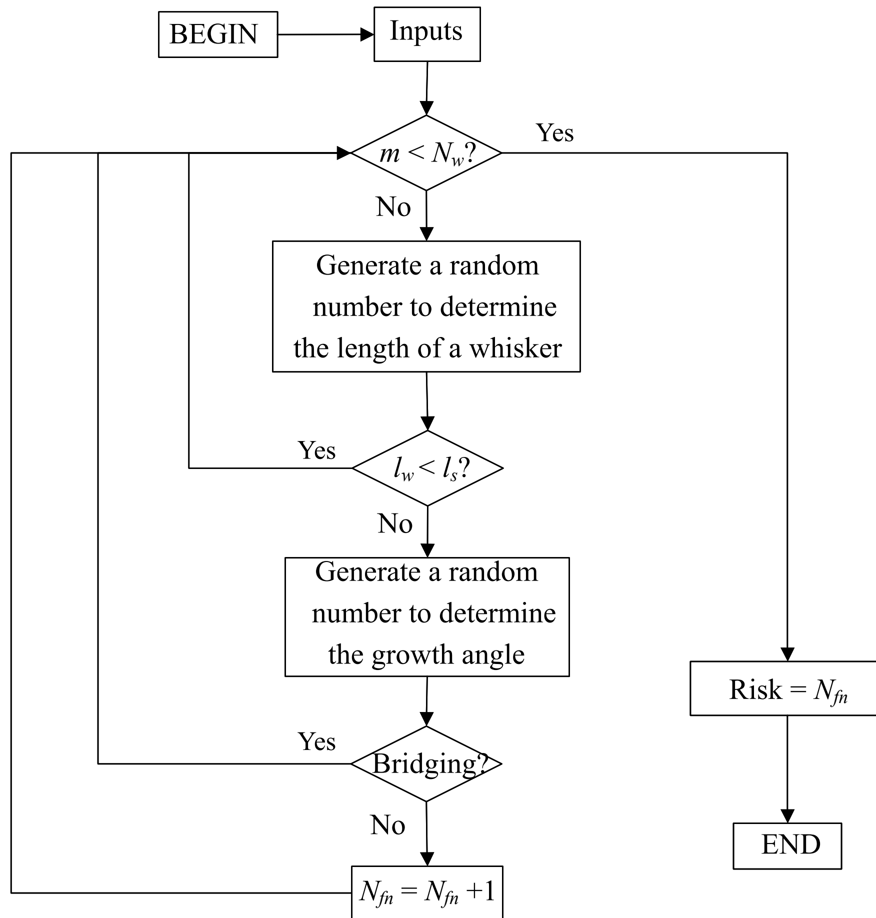

Figure 4.4 Flowchart of fixed risk assessment (II)

If Monte Carlo simulation is applied to assess occurrence of the bridging numbers for a given application, as illustrated in Figure 4.5, the distribution of occurrence of the possible bridging numbers can be quantified. Theoretically, the bridging numbers can vary from zero to infinity. Thus we know, for example, the probability that 2 bridging occur for an application.

In the flowchart, $N_f[N_{mc}]$ is an array whose dimension is equal to the sample size of Monte Carlo simulation. This array is used to record the number of occurance of the bridging number in each simulation.

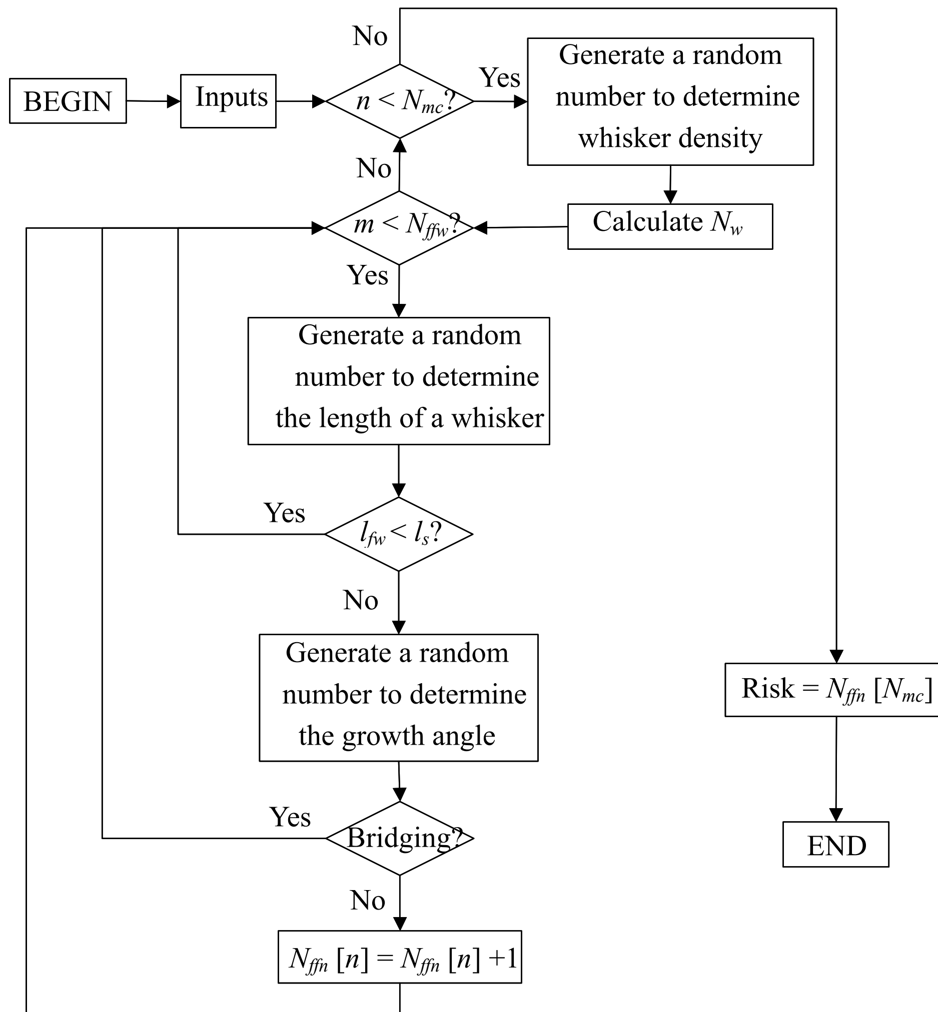

Figure 4.5 Flowchart of fixed risk assessment (III)

4.2.5 An example of implementation for fixed risk

As mentioned, bright tin always produces more and longer whiskers than matte tin. Furthermore, bright over brass was shown the worst combination. As a conservative case, information of whisker growth on bright tin over brass was used to assess tin whisker risk. An example of risk assessment is presented below.

For this example, a tin finished small outline package (SOP), is considered. The SOP is assumed to have a brass lead-frame plated with bright Sn. Whisker growth

data discussed in Chapter 3 was used in this case. The geometry data of the packages are presented in Table 4.1.

Table 4.1 Geometry parameters of the SOPs

Number of leads on a package	Surface area of a lead (mm^2)	Surface area of all the leads on a package (mm^2)	Spacing between adjacent conductors (mm)
14	2.3	32.2	0.15

As discussed in Chapter 3, three measurements on whisker growth on the sample of bright tin over brass have been conducted until the 18th month of room ambient storage. Then how to obtain the information after the 18th month based on the measured data? For this case, whisker density and mean length were predicted using the growth rates in the 18th month. This is conservative since whisker growth was decreasing – the growth rate afterward should be less than in the 18th month. The distributions of the growth parameters are shown in and Table 4.2.

Table 4.2 Predicted distributions of the growth parameters [23]

<table>
<tr><td>Whisker growth parameter</td><td>Density distribution</td><td>Length distribution</td><td>Growth angle distribution</td></tr>
<tr><td>Distribution</td><td>Normal</td><td>Lognormal</td><td>Step-wise uniform</td></tr>
<tr><td>Distribution parameters at the 33rd month of storage</td><td>m = 14520/cm^2
sd = 3180</td><td>m = 27.2 μm
sd = 11.4</td><td rowspan="3">$f(\alpha)=\begin{cases}0.0035 & 0\le\alpha<20\\ 0.0072 & 20\le\alpha<40\\ 0.0122 & 40\le\alpha<60\\ 0.0180 & 60\le\alpha\le 90\end{cases}$
(α: growth angle in degree)</td></tr>
<tr><td>Distribution parameters at the 53rd month of storage</td><td>m = 15280/cm^2
sd = 3180</td><td>m = 28.4 μm
sd = 11.4</td></tr>
<tr><td>Distribution parameters at the 78th month of storage</td><td>m = 16080/cm^2
sd = 3180</td><td>m = 29.9 μm
sd = 11.4</td></tr>
</table>

For this case, whisker growth is approaching the saturation point. What if whisker growth is not approach the saturation point? Than the average of growth rates

between two measurement periods can be used to predict growth parameters. However, the prediction should keep updated by the newest data to make the prediction more accurate.

As an example of the simulation for the 18th month whisker density, if a random number 0.6 is generated in the first Monte Carlo simulation, the density is then 15326/cm^2, calculated from the inversed density distribution function. The number of the whiskers formed on this SOP is 4934, which is the product of whisker density and the surface area of the leadframes. The next step is to simulate whisker length and growth angle for these 4934 whiskers one by one until a bridging short occurs or until the last whisker if resulting in no bridging.

The first simulation for the 4913 whiskers is depicted in Table 4.3. The simulation for the first whisker is terminated after its length is sampled. This is because the simulated whisker length is smaller than the spacing of adjacent conductors, which means no bridging risk for this particular whisker. Then the simulation jumps to sample the second whisker. It can be seen that no failure occurs in this first Monte Carlo simulation since all the 4934 whiskers are sampled.

Table 4.3 Simulation procedure (I)

Whisker number	Length of whiskers (mm)	Growth angel (°)	Short occurs?
1	0.16	-	-
2	0.42	31.7	No
3	0.36	-	-
…	…	…	…
4934	0.12	-	-

The simulation then goes to the second Monte Carlo simulation after the first

one is accomplished and repeated the same procedure. If a random number 0.35 is generated for whisker density, the density is 13294/cm^2 and the number of the whiskers is 4281. The simulation results are shown in Table 4.4. As shown in the Table, this simulation is terminated at the third whisker since this whisker causes a bridging failure. Then the simulation goes to the third simulation. Similarly, the Monte Carlo simulation continues until the 3000th simulation.

Table 4.4 Simulation procedure (II)

Whisker number	Length of whiskers (mm)	Growth angel (°)	Short occurs?
1	0.19	-	-
2	0.39	13.9	No
3	0.51	80.3	Yes
4	-	-	-
…	-	-	-
4281	-	-	-

In order to avoid over conservation, it is recommended to integrate the maximum length into the algorithm and use the truncated lognormal distribution. For this case, the largest whiskers in length were 98, 132 and 147 for 8th, 13th and 18th month respectively and truncated whisker length distribution is applied as the upper limit of the lognormal distribution at each specific time. The truncated distribution is not used after the 18th month since the maximum length is unknown and impractical to predict.

The input data for spacing between adjacent conductors are 0.15, 0.20 and 0.25 mm in order to demonstrate the effect of spacing on tin whisker risk. The results of this case are shown in Table 4.5. It can be seen that spacing affects tin whisker risk

significantly.

Table 4.5 Simulation risk with time

Duration (month)		0	13	15	18	33	53	78
Risk (%)	s = 0.15 mm	0	0	0	0.9	3.8	6.5	11.6
	s = 0.20 mm	0	0	0	0	0.1	0.2	0.5
	s = 0.25 mm	0	0	0	0	0	0	0

The values presented in Table 4.5 are the nominal values because the bridging risk calculated by the algorithm varies for each time given the same conditions. The simulation results also follow a distribution. It was found that normal distribution is the best fit.

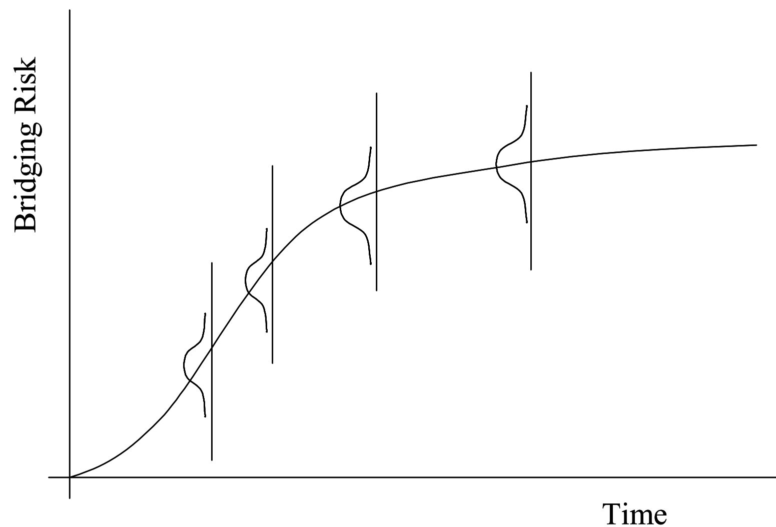

Figure 4.6 Bridging simulation risk with time

As an example, spacing 0.20 mm at the 53rd month has been simulated for 50 times. The mean was 6.5% and the standard deviation was 1.1%. The bridging simulation risk posed by fixed whiskers with time is illustrated in Figure 4.6. After the distribution is quantified, the percentile of bridging risk can be determined. For this

case, it can be said that the bridging risk, with 90% change, is small than 7.9%.

In this simulation, there is only one type of conductors – the leads on the part of SOP. If there is more than one part, the risk for this type can be estimated by

$$P_{Risk}^{i} = 1-(1-P_{Ri})^{n_i} \qquad (4.3)$$

where i is part type; n_i is the number of parts of the ith type; P_{Ri} is the risk for one package of the ith type; and P_{Risk}^{i} is the total risk for all the parts of the ith type.

If there is more than one type of parts are in a product, the total risk for the product is

$$P_{Product} = 1-\prod_{j=1}^{m}(1-P_{Risk}^{j}) \qquad (4.4)$$

where m is number of part type; n_i is the number of $P_{Product}$ is the total risk posed by whiskers on the product.

Table 4.6 Results of bridging number distribution

Bridging number	0	1	2	3	4
Number of occurrence	2806	188	6	0	0
Percentage (%)	93.53	6.27	0.20	0	0

As an example, bridging number distribution is simulated for the 53rd month. The results are presented in Table 4.6. It can be seen that bridging occurs only one or two times for the SOP until 53 months of storage. Given that a bridging failure occurs, one time of failure dominates. The summarization of the probability of one bridging and the probability of two bridging is risk of bridging failure shown in Table 4.5.

4.3 Risk Assessment for Free Whiskers

In this section, failure definition of bridging failure risk introduced by fixed

whiskers is defined and the procedure of the risk assessment is developed.

4.3.1 Failure definition

As presented in Figure 4.7, a failure occurs immediately if this condition is met:

$$l_{fw} \cdot Sin(\alpha) \geq l_s \qquad (4.5)$$

where α is whisker deposition angle, l_{fw} is the length of the deposited broken free whisker, and l_s is the spacing between the adjacent exposed conductors. Similar to the definition of fixed risk, the failure definition does not consider the consequences of the bridging and can be applied to any shape of exposed conductors not only for parallel conductors.

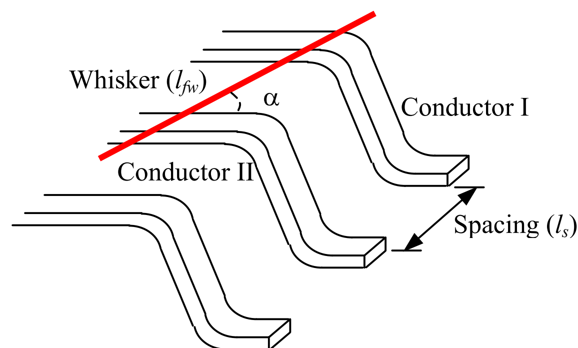

Figure 4.7 Bridging short caused by free whiskers

4.3.2 Characteristic parameters related to free whiskers

The characteristic parameters of broken free whiskers include free whisker density in air, length, deposition angle, and probability of deposition on the exposed conductors.

Probability of deposition on the exposed conductors refers to the likelihood of

a whisker depositing into the area where exists exposed conductors. Deposition angle, as illustrated in Figure 4.7, is the angle between the length orientation of a whisker and the orientation of a conductor.

Similar to whisker growth the characteristic parameters are also expressed in distributions. The methods to collect the information of characteristic parameters will be discussed Chapter 5.

4.3.3 Assessment algorithm to quantify bridging risk in terms of risk probability

Similar to the bridging fixed risk assessment procedure, the bridging free risk assessment procedure also consists of inputs, simulation calculation and output. The inputs include the characteristic parameters, the geometry parameters, and the initial variables and control variables. The initial variables include the number of failures which is set as zero initially, and sample size of Monte Carlo simulation. The output is the failure risk at a specific time.

The procedure to assess free bridging risk is illustrated in Figure 4.8. Four random variables are generated to sample whisker density, the length of a whisker, the deposition site of the whisker, and the deposition angle of the whisker.

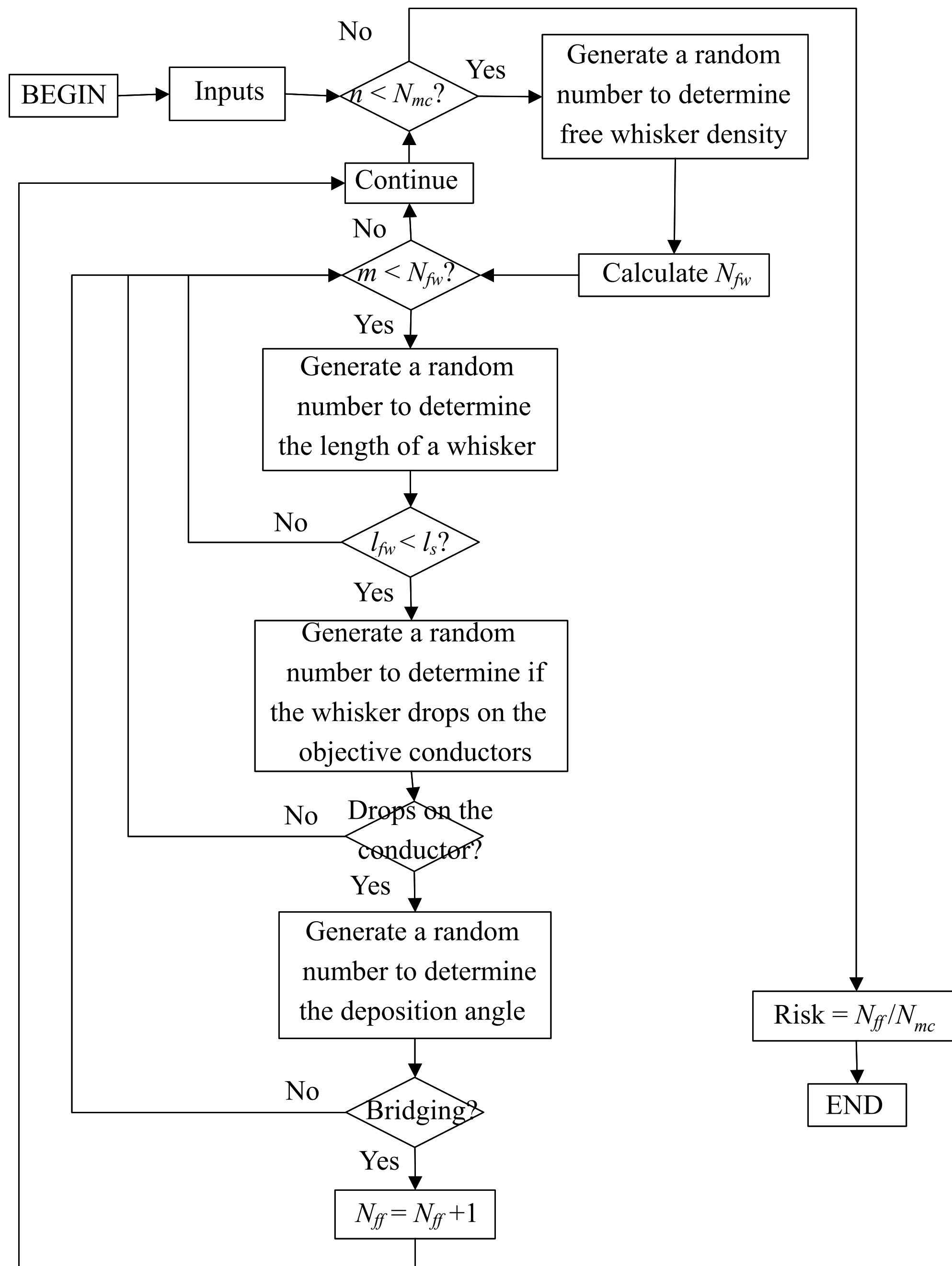

Figure 4.8 Procedure of free risk assessment (I)

In the procedure, N_{ff}, N_{mc}, l_{fw}, l_s, and N_{fw} are the number of bridging shorts, the sample size of the Monte Carlo simulation, the length of a sampled whisker, spacing of the adjacent exposed conductors, and the number of whiskers in a simulation; while n and m are the iterative control numbers for Monte Carlo simulation and the sampled

broken whiskers. N_{ff}, the number of bridging failure, will increase one if a failure occurs during the simulations.

The simulation will go to the next simulation if the first bridging occurs in order to avoid double counting a failure and save computing time because the product will fail immediately once the first bridging short occurs, which means it is not needed to examine if any extra failure(s) caused by others whiskers. The final bridging free risk posed by broken free whiskers to a product is:

$$R_{free} = N_{ff} / N_{mc} \qquad (4.4)$$

4.3.4 Assessment algorithm to quantify risk in terms of bridging number for free whiskers

For a standby electronic product, the likelihood of failure of a product will increase when it is activated if the number of bridging shorts increases. The procedure of the assessment algorithm to quantify the number of bridging shorts is illustrated in Figure 4.9. The inputs and the variables have the same meaning as the previous ones except N_{ffn}, which is the number of bridging shorts. The output N_{ffn} is the nominal bridging number.

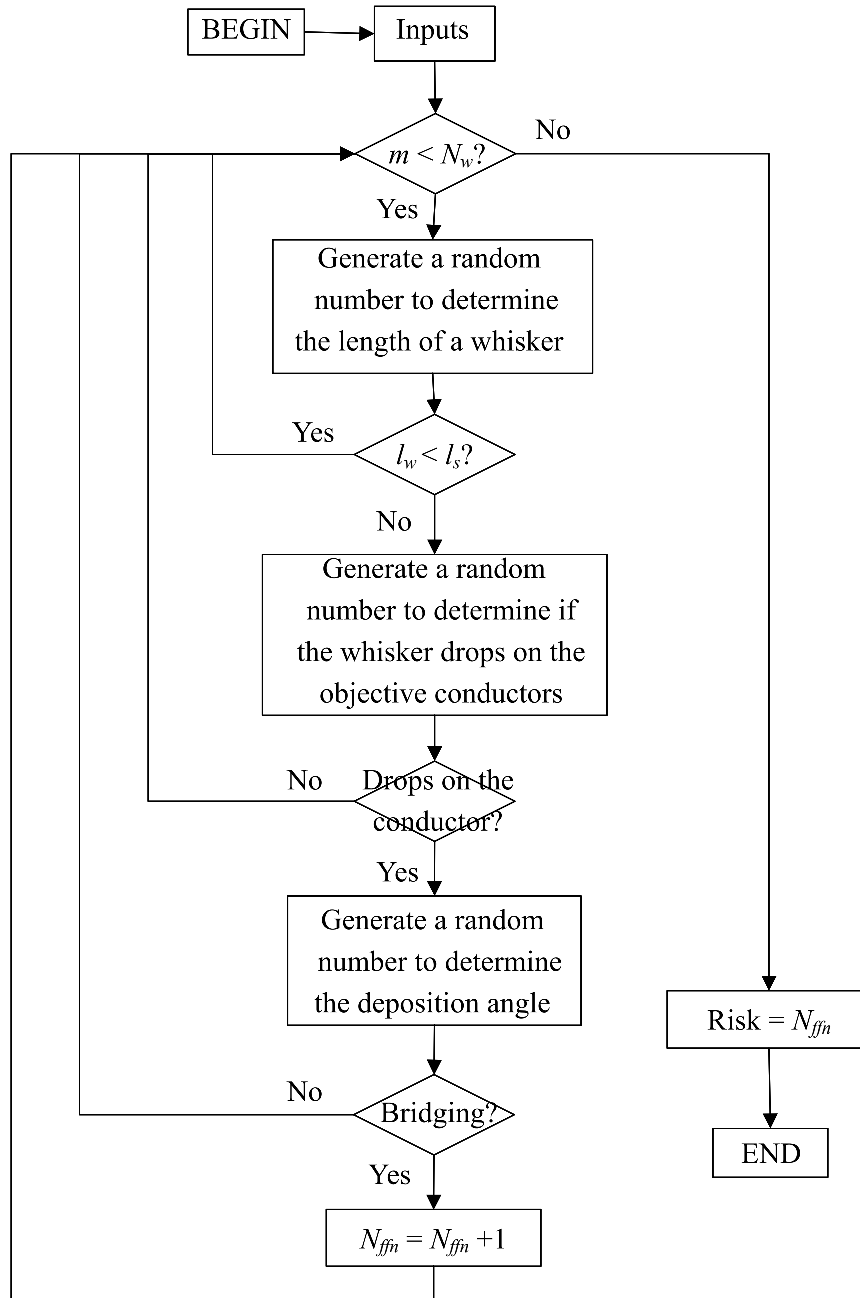

Figure 4.9 Procedure of free risk assessment (II)

If Monte Carlo simulation is applied to assess occurrence of the bridging numbers for a given application, as illustrated in Figure 4.10, the distribution of occurrence of the possible bridging numbers can be quantified. In the flowchart, $N_{ff}[N_{mc}]$ is an array which has the same size of dimensions as the sample size of Monte Carlo simulation. This array is used to save the bridging numbers for each

simulation and serves as the output.

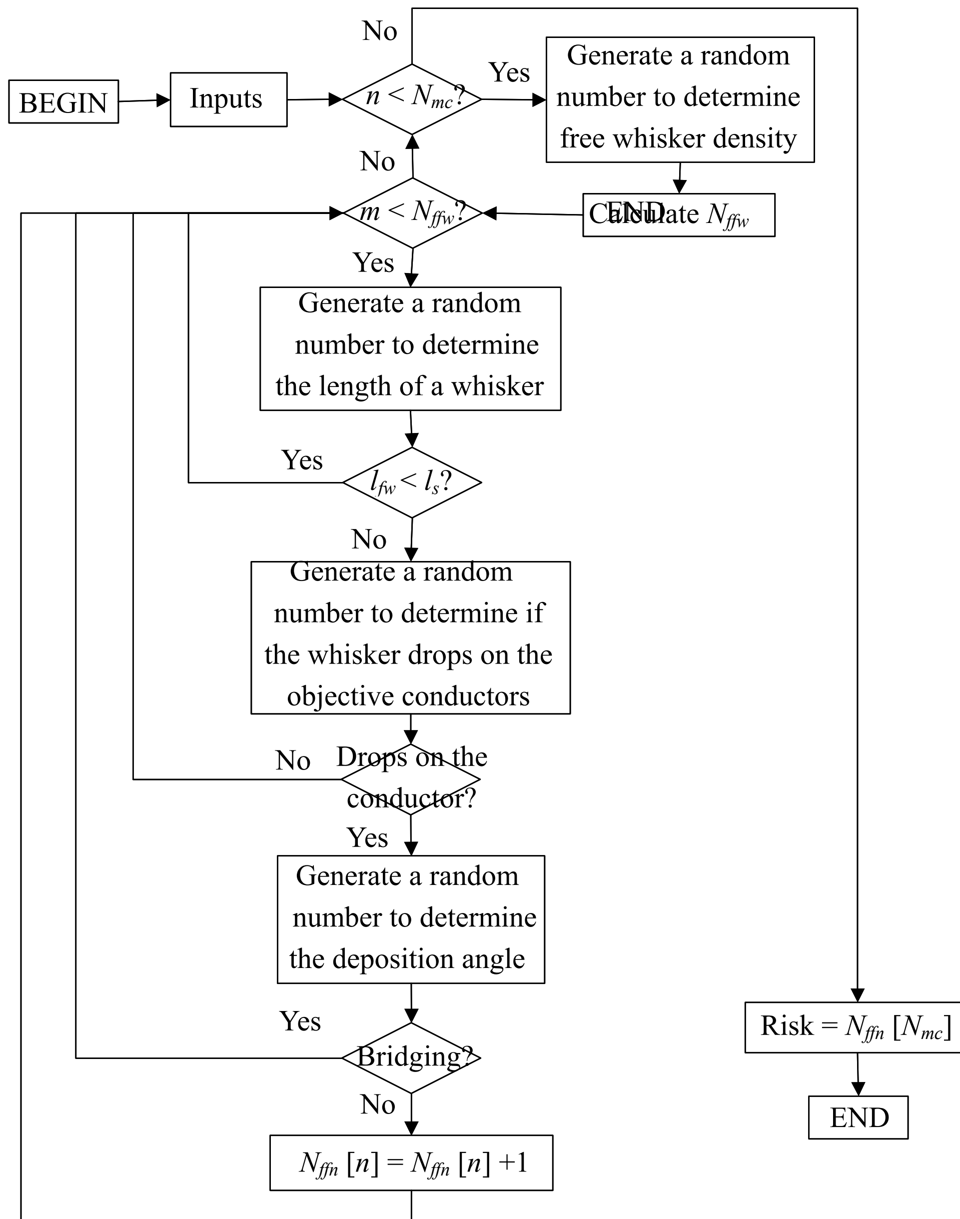

Figure 4.10 Procedure of free risk assessment (III)

4.3.5 An example of implementation for free whiskers

The simulation objective is a rectangular printed wiring board (PWB) with 40 small outline (plastic) packages (SOPs). The board is installed in a box which is considered a control volume and has the same shape and area as the PWB. A fan is

installed on a sidewall and airflow volume velocity is 10 cm^3/sec. The box is placed in the environment with broken free tin whiskers flowing with air. For this case, the bridging failure risk is only from external broken free whiskers.

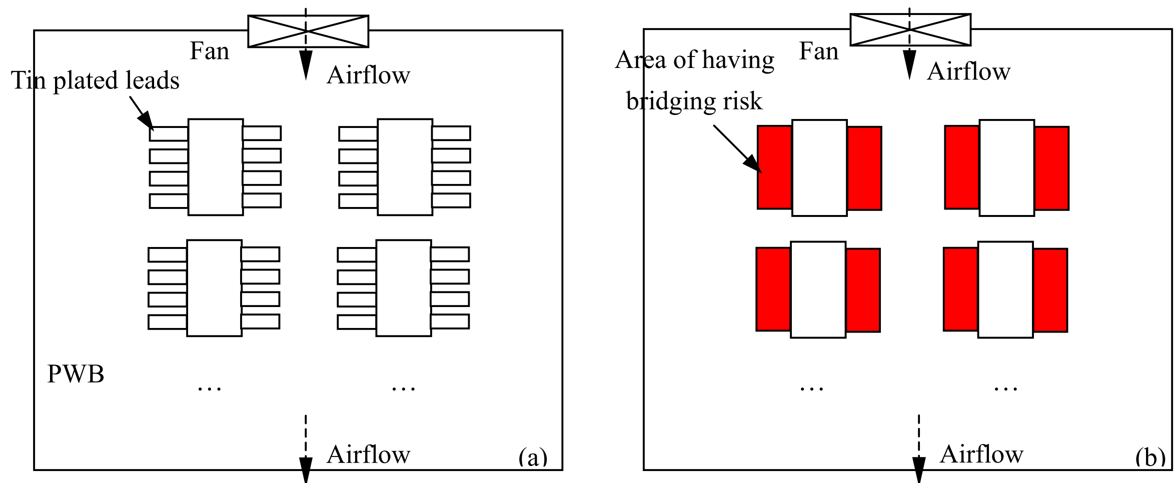

Figure 4.11 Arrangement of parts on the printed wiring board

Table 4.7 Distributions of relevant parameters of free whiskers

Relevant parameters	Density distribution	Length distribution	Distribution of depositing on conductors	Deposition angle distribution
Distribution	Normal	Lognormal	Uniform	Uniform
Distribution parameters	$\mu = 8000/m^3$ $\sigma = 3000$	m = 26.0 μm $\sigma = 11.4$	0.0330	1/90

The SOPs are lined 20 rows and uniformly distributed from the wall with the fan to the opposite wall, as shown in Figure 4.11 (a). Each row has two parts. The spacing between adjacent conductors on a SOP is 0.150 mm and the smallest gap between nearest conductors of the neighboring SOP is 3 mm. Based on the distribution parameters shown in Table 4.7, the likelihood of the length of a whisker larger than 1 mm is almost zero. Therefore, only the leadframe area of the SOPs have

bridging risk posed by free risks. The leadframe area under free risk is 3.30 cm^2 as shown in Figure 4.11 (b).

As presented in Table 4.7, the distribution for deposition site follows step-wise uniform. Air is pushed by the fan into the control volume and airflow distribution and velocity are different at different zones in the control volume. This affects deposition site of a whisker given it deposits on the floor of the box. Accordingly, the box floor is equally divided into four zones from the wall with the fan to the opposite wall to simulate the deposition site influence. In each zone, the probability of a whisker depositing in the conductor area is the ratio of the conductor area in the zone and the zone area.

For this case, the 40 identical SOPs are uniformly distribution on the PWB. The ration of conductor area and the zone area is same for each zone no matter the shape and area of each zone; and thus the probability of a whisker depositing in the conductor area is equal for each zone. Therefore, the probability of a whisker depositing in the conductor area is the ration of the whole conduction area and the area of the PWB. It should be noted that the likelihood of a whisker dropping into the zones is different. But whichever zone it drops, the probability of depositing in the conductor area for this whisker is the same.

The sample size of the Monte Carlo iteration in this simulation is 3000. Bridging risk posed by broken free whiskers is a dynamic procedure since whiskers are cumulating in the control volume with time. The volume of airflow into the control volume is 864000 cm^3/day since airflow velocity is 10 cm^3/sec.

As an example to calculate the bridging risk, if a random number 0.7 is generated for whisker density in the first Monte Carlo simulation, the broken free whisker density should be 9573/m^3, calculated from the inversed density distribution function. To be conservative, all the whiskers entered the control volume are assumed to deposit on the floor if information of the percentage of whiskers escaping out of the control volume is not available. For this case, the number of whiskers deposited on the box floor per week is 57898 and the number of whiskers dropped into the exposed conductor area is 1910. The next step is to simulate whisker length, and deposition angle for these 1910 whiskers one by one until a bridging short occurs or until the last whisker if no bridging occurs.

The simulation goes to the second simulation after the first is finished and repeated the same procedure. Then the Monte Carlo simulation continues until the 3000th simulation. The output is the risk at the end of the first week. Risk at the end of the second and second forward can be estimated by

$$P_{Risk}^{n} = 1-(1-P_R)^n \qquad (4.5)$$

where n is the number of period in week for the ith type; P_R is the risk in the first week; and P_{Risk}^{n} is the risk in the nth week. The results of this case are presented in Table 4.8.

Table 4.8 Simulated risk of the SOP with time

Duration (week)	0	1	5	10	20	25	45
Risk (%)	0	0.43	2.2	4.3	8.3	14.1	17.7

If more than one type of parts in an product, the overall risk of the product with time can be estimated by

$$P^{n}_{Product} = 1 - \prod_{i=1}^{m} (1 - P^{n_i}_{Risk}) \qquad (4.6)$$

where j is part type; and m is the number of part type.

4.4 Integration of Fixed and Free Risks

The overall bridging risk posed by tin whiskers can be obtained after the fixed and free bridging risks are evaluated. It is assumed that fixed and free bridging risks are independent. Then the overall bridging risk is

$$R_{or} = 1 - (1 - R_{fixed}) * (1 - R_{free}) \qquad (4.7)$$

where R_{or}, R_{fixed} and R_{free} are overall bridging risk, fixed and free risks on a product respectively.

An electronic product may not be exposed to both fixed and free bridging risks simultaneously or one of two bridging risk is negligible. This is one of the reasons that the algorithms of fixed risk and free risk are developed separately.

4.5 Effectiveness of Mitigation Strategies and Cost

As mentioned in the previous chapters, in order to retard or eliminate tin whiskers formation in the pure tin or high tin lead-free alloy finished surfaces, various mitigation strategies [45][50] have been proposed. Effectiveness of the mitigation strategies was usually evaluated in terms of change of whisker density and the maximum whisker length, with and without applying the strategies. However, this was a qualitative analysis since it did not offer a quantitative answer.

The algorithm developed in this study can provide a quantitative evaluation on effectiveness of the mitigation strategies since it can quantify the bridging risks for the situation of without and with applying the strategies. The difference between the risk values is the effectiveness of a strategy. Also effectiveness of different strategies can also be evaluated. The bridging risks, after the strategies have been applied respectively, can be quantified. The effectiveness of the various strategies can be evaluated by comparing the risk values related to the corresponding strategies.

Chapter 5 Simulation Experiments

Two experiments are designed and conducted to simulate bridging failures introduced by fixed and broken free whiskers; whereas the previous experiments related to metal whisker mainly focused on whiskering propensity. Methods to collect information of the risk parameters are discussed. Error analysis for the difference of simulation and experimental results is also provided in this chapter.

5.1 Experimental Design for Fixed Failure Risk

This experiment is especially designed to simulate the bridging failures caused by fixed tin whiskers.

5.1.1 Experimental vehicles and conditions

The coupons used in this experiment was bright tin plated over brass since this combination may grow more and longer whiskers in shorter period of time compared to other combinations, according to the previous studies.

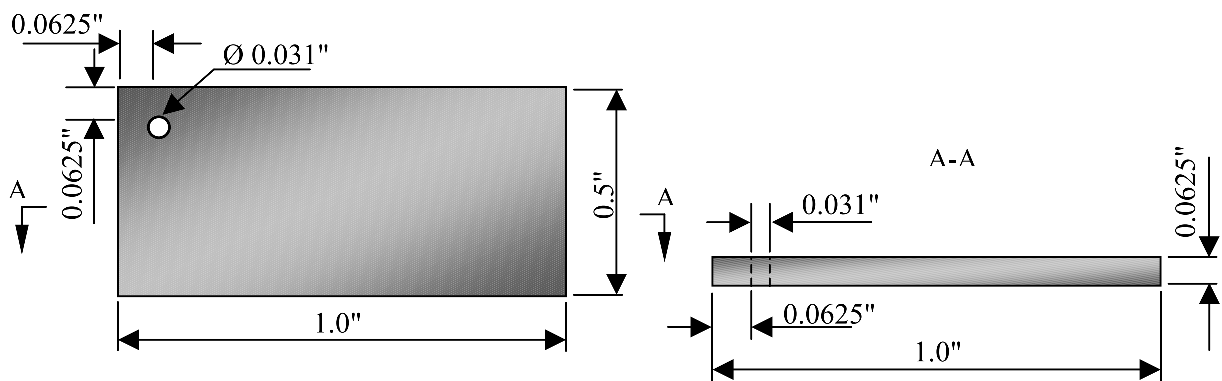

Figure 5.1 Configuration of a experimental coupon

The configuration of a coupon was illustrated in Figure 5.1. The length, width and thickness were 1.0", 0.5" and 0.625" respectively. There was a hole with the diameter of 0.031" at a corner of the coupons, which facilitated to plate pure bright tin. The thickness of the tin finish was 5±0.8 μm.

Two coupons, separated by two insulators at the two sides, were paired together to form an experimental set. The experimental surfaces, in which tin whiskers developed, were the two opposite inner two surfaces of the coupons, as shown in Figure 5.2. The size of an experimental surface was 0.5"×0.5".

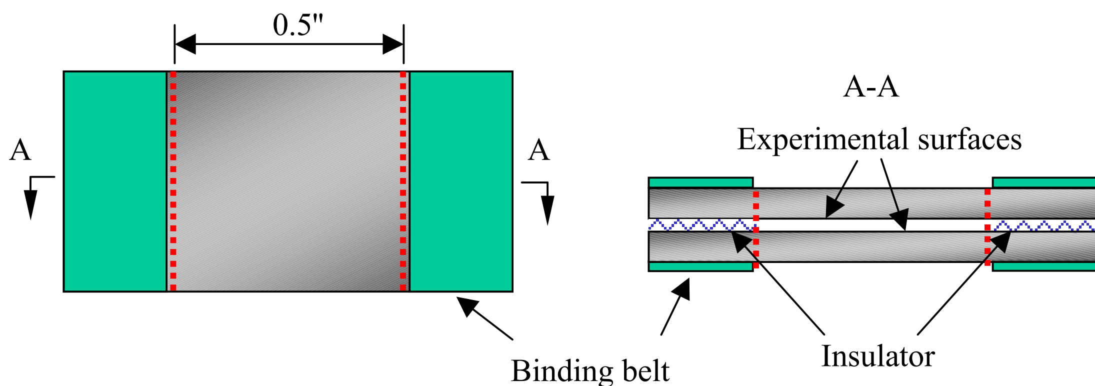

Figure 5.2 Configuration of an experimental set

The experimental sets were divided into two categories of experimental sets: non-conformal coated and conformal coated sets. For the coated sets, only the internal experimental surfaces were coated. The materials of the conformal coating were urethane and parylene. Thus there were three groups of sets: non-coated, urethane-coated and parylene-coated sets with the sample sizes of 40, 30 and 30 respectively. The nominal thickness of the conformal coating for both urethane and parylene was 100 μm. Different insulators were used for the non-coated and coated

set. 75-µm-thick films were used to separate the non-coated sets and 25-µm-thick films on the conformal coated sets. All the experimental sets were stored in temperature/humidity (50°C/50%RH) after one week of plating.

The insulators were Kapton film of type 100NH and 300 NH, with the thickness of 25 and 75 µm. Based on the manufacturer provided information [19], the Kapton films will keep excellent physical, thermal, electrical, and chemical properties in the conditions of temperature/humidity (50°C/50%RH) used in this study.

A bridging failure occurs when at least one whisker growing in an experimental surface reaches the opposite surface. Resistance was selected as the parameter to monitor if a bridging short occurs among the sets. An ohm meter has been used to monitor the resistance. Without bridging, the sets were open and resistance between the two coupons was infinity. The resistance dropped dramatically down to less than 10 ohms when the set was bridged by some fine materials, such as carbon fibers. A 1000-ohm resistor of was connected serially to the ohm-meter when measuring the sets resistance in order to protect the whiskers from melting due to the unintended large electrical current. The set will be removed if it results in a bridging failure.

Two un-paired identical coupons for each of the three groups were also stored in the same T/H environment in order to monitor whisker growth. Whisker growth data has been collected from those coupons.

5.1.2 Results of the experiment

The non-coated and coated sets have been stored in the temperature/humidity

chamber for five and four month respectively. Four measurements of whisker growth on the non-paired reference coupons have been conducted. Lognormal and normal distributions were still applied to fit the data for whisker length and density. The measurement and fitting results of the non-coated sets are presented in Table 5.1.

Table 5.1 Whisker growth measurement results of the non-coated sets

Duration (month)	1.5	3.0	3.5	5
Length distribution: lognormal parameters (μm)	m = 3.81 sd = 1.66	m = 8.05 sd = 4.37	m = 10.8 sd = 5.03	m = 13.72 sd = 6.50
Maximum length (μm)	10.5	24.8	30.1	35.2
Density distribution: normal parameters (#/cm^2)	m = 75 sd = 73	m = 97 sd = 71	m = 106 sd = 77	m = 121 sd = 86

Whisker growth angle was also measured and the results are presented in Table 2.1. Step-wise uniform distribution is used to describe whisker growth angle preference. Based on the collected data, growth angle is fitted to distribute uniformly in three ranges: 0 to 50, 50 to 80, and 80 to 90 degree.

Table 5.2 Growth angle distribution

Angle range (°)	0~10	10~20	20~30	30~40	40~50	50~60	60~70	70~80	80~90
Percentage (%)	2.0	6.1	8.2	4.1	6.1	20.4	18.4	24.5	10.2

Based on the growth rates from 3.5 to 5 months, whisker average density and mean length were predicted, as shown in Table 5.3. The corresponding bridging risks at each specific time were also predicted.

Table 5.3 Prediction of whisker growth and the corresponding bridging risk

Duration (month)	5	10	15	25
Length distribution: lognormal parameters (mm)	m = 13.7 sd = 6.5	m = 23.1 sd = 9.9	m = 32.4 sd = 12.5	m = 51.1 sd = 16.5
Density distribution: normal parameters ($\#/cm^2$)	m = 121 sd = 86	m = 172 sd = 111	m = 221 sd = 131	m = 322 sd = 164
Simulation risk (%)	0.0	20.0	73.5	97.0

In the process of calculating the simulation risk with time, truncated normal distribution has been used to guarantee whisker density always larger than zero because for this case, the values of the average densities and standard deviations were close to each other and the percentile of density less than zero was not negligible.

A truncated normal distribution is a normal distribution that is restricted within a range, $A \le x \le B$, where A and B are the lower and upper truncation limits. A and B can be negative or positive infinity, but not both at the same time. The truncated probability density function (PDF) of normal distribution [12][57] can be expressed as:

$$f(x,a,b,\mu,\sigma) = \frac{\phi(\frac{x-\mu}{\sigma})}{\sigma[\Phi(\frac{b-\mu}{\sigma}) - \Phi(\frac{a-\mu}{\sigma})]} \qquad a \le x \le b \qquad (5.1)$$

where μ and σ are the mean and standard deviation of the parent normal distribution; a and b are the lower and upper truncation limits; ϕ and Φ are the PDF and cumulative distribution function (CDF) of normal distribution.

The truncated normal cumulative distribution [12][57] can be expressed in terms of the standard normal cumulative distribution function as follows:

$$F(x,a,b,\mu,\sigma)=\frac{\Phi(\frac{x-\mu}{\sigma})-\Phi(\frac{a-\mu}{\sigma})}{\Phi(\frac{b-\mu}{\sigma})-\Phi(\frac{a-\mu}{\sigma})} \qquad a\le x\le b \qquad (5.2)$$

In this case, a is zero and b is positive infinity and therefore the PDF of $\Phi(\frac{b-\mu}{\sigma})$ is 1. The CDF is

$$F(x,a,b,\mu,\sigma)=\frac{\Phi(\frac{x-\mu}{\sigma})-\Phi(\frac{-\mu}{\sigma})}{1-\Phi(\frac{-\mu}{\sigma})} \qquad 0\le x<\infty \qquad (5.3)$$

For whisker density (75, 73) at 1.5 month, for example, the percentile $\Phi(\frac{-\mu}{\sigma})$ from negative infinity to 0 is 0.152. Therefore, the equation is

$$F(x,a,b,\mu,\sigma)=\frac{\Phi(\frac{x-\mu}{\sigma})-0.152}{0.848} \qquad 0\le x<\infty \qquad (5.4)$$

In the process of generating a random number for whisker density, F is the random number and $\Phi(\frac{x-\mu}{\sigma})$ is the corresponding CDF value for the non-truncated normal distribution. The corresponding density value can be calculated using the inversed normal distribution; and thus whisker density is always larger than zero.

$$\Phi=0.152+0.848\cdot F \qquad 0\le x<\infty \qquad (5.5)$$

Correlation among whisker density, length and growth angle has also been examined on the collected data. The correlation between length and growth angle was estimated using the equation [5]:

$$r_{x_j,x_k}=\frac{\sum_{i=1}^{n}(x_{ij}-\bar{x}_j)(x_{ik}-\bar{x}_k)}{[\sum_{i=1}^{n}(x_{ij}-\bar{x}_j)^2\sum_{i=1}^{n}(x_{ik}-\bar{x}_k)^2]^{1/2}} \qquad (5.6)$$

where x_j and x_k are the values of length and growth angle of a whisker; n is the number of the observed whiskers. For whiskers measured in the 5th month, the value of correlation was –0.186, which indicates a weak relationship of whisker length and

growth angle. Therefore, whisker length and growth angle can be considered independent. The relationship of whisker density and growth angle is independent since density increases with time while growth angle is independent of time. It may not be practical to quantify the correlation value of whisker density and length since the ways to measure these two parameters are different. Based on the previous observation for different coupons and applications and the current data, the relationship of density and length is still inconclusive.

As can bee seen, the prediction of both whisker growth and the bridging risks appears large, compared to the real collected data discussed in Chapter 3. This may be due to the inaccurate extrapolation. The period to collect whisker growth information is within 5 month. According to the previous information collected for bright tin plated over brass discussed in Chapter 3, whisker growth approached the saturation point until after 18 months. Though the testing conditions were different for the two experiments, information within a period of 5 months may not be sufficient to make an accurate prediction.

This is situation is illustrated in Figure 5.3. If information within 5 months is used to predict whisker growth, the prediction (dashed line) will be much larger than the real growth; and consequently the simulation bridging risk is also over-estimated. In order to minimize inaccurate prediction, it is recommended to update the prediction using the newest data and use real data to estimate the current bridging risk caused by fixed whiskers.

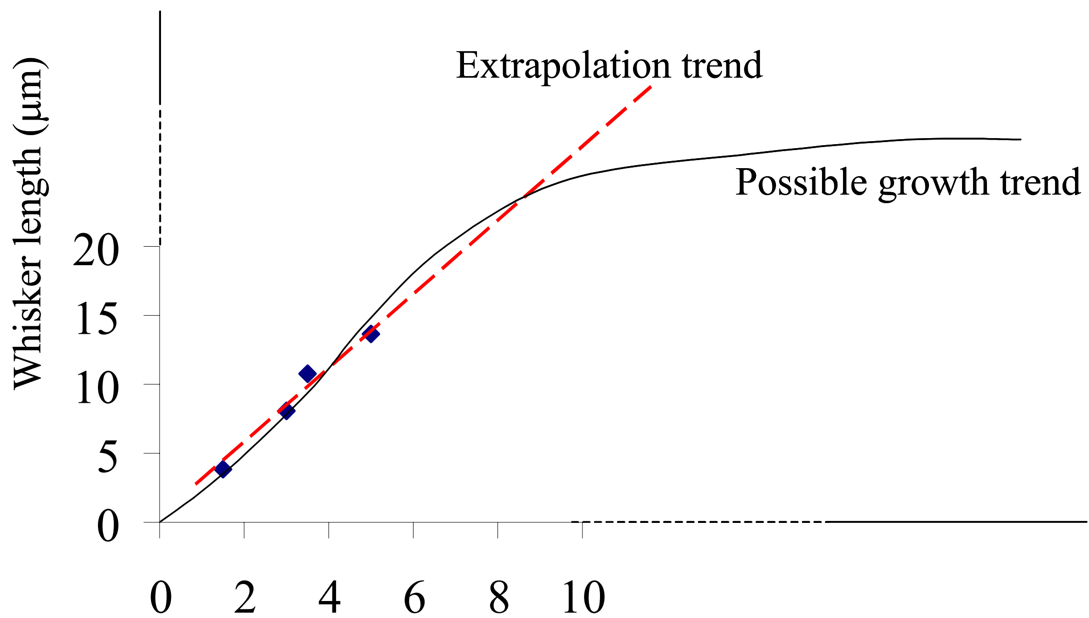

Figure 5.3 Whisker growth with time

Whisker growth observations on the reference conformal-coated coupons have also been conducted for four times. But the observations had some limitations. The E-SEM was not able to observe the tin finished surface since the electrons of the E-SEM can penetrate 5 to 10 into the coating, whereas the thickness of the conformal coating was 100 microns. The optical microscope is also not capable since it has no enough high magnification.

Only the conformal coating surfaces have been observed. No whiskers have been found to penetrate the coating and no dome-shape sites have been detected. A dome forms if a whisker in the conformal coating grows long enough and pushes the coating towards the coating surface.

All the experimental sets have being monitored once a week to check if any bridging shorts occurred. No bridging shorts have been detected until the 5th month

storage period. The simulated results, obtained by inputting the information in Table 5.1 into the risk assessment algorithm, have also shown zero failure.

5.2 Experimental Design for the Free Risk

This experiment is especially designed to simulate the bridging failures introduced by broken free whiskers.

5.2.1 Experimental vehicles

The experimental vehicle was a fine-pitch quad flat package (QFP). There were 176 leads on the QFP with each side having 44 leads equally. The spacing between adjacent leads was 0.242±0.014 mm. The plastic molding compounds of the QFP were ground and polished in order to disconnect the wire bonds inside the package to make the leads open.

Resistance between two adjacent leads was selected as the parameter to judge if a bridging short occurs. The resistance was infinite because they were open. The pre-completion test showed the resistance dropped down significantly from infinity to below 100 ohms if a carbon fiber bridged the two leads. The resistance will also drop significantly if a whisker bridging two adjacent leads. Because this was a dynamic test, all the leads were wired and connected to the data-loggers to have the in-situ monitoring on the resistance. The data-loggers were connected the computer to have the data of resistance recorded automatically. The schematic of the experimental design is shown in Figure 5.4.

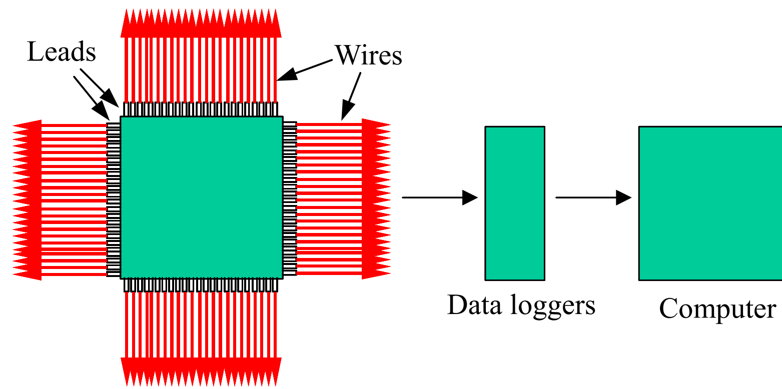

Figure 5.4 Conceptual configuration of experimental vehicle

The QFPs with the wiring was installed in a rectangular transparent plastic box. The dimension of the box was 12.5×12.5×9 cm in length, width and height. Five holes were made on the five walls. There was a hole of 10×10 cm on the top wall for dropping broken whiskers onto the PCB. Each sidewall had a hole; three of them was 10×2 cm for facilitating the wires out of the box.

5.2.2 Design of data collection

The method to collect the information of the broken free whisker characteristic parameters is illustrated in Figure 5.5. For each test, five copper tapes with size of 1×1 cm were used to trap deposited whiskers. One tape was laid on top of the QFP and four tapes were laid around the QFP.

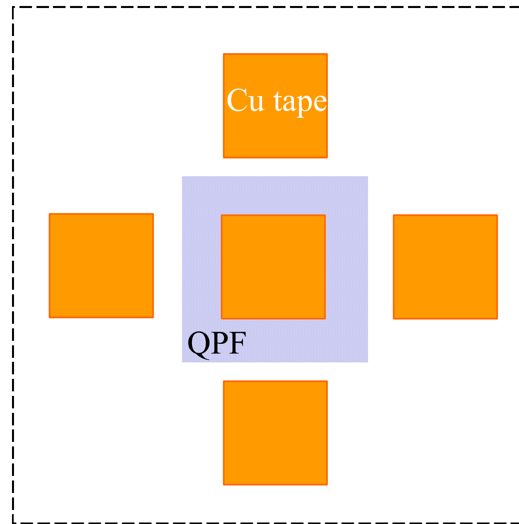

Figure 5.5 Design for quantifying the characteristic parameters

Same procedure, as discussed in Chapter 3, have been used to observe and fit the distribution for the deposited broken free whiskers. In this experiment, zinc whiskers were uniformly controlled in the area of 6×6 cm. Whisker density on each Cu tape was also used to check if whiskers uniformly dropped.

5.2.3 Experimental and simulation results

Totally 17 tests have been conducted and the data showed that whiskers have been uniformly distributed. Average whisker density on the tapes was 14 $\#/cm^2$ with the standard deviation of 3 and longest whisker found was 853 µm. Whisker mean length was 166 µm with the standard deviation of 208. Deposition angle was uniformly distributed. Three bridging shorts were detected among the 17 tests. The risk was 0.176.

Simulation risk was calculated based on the information of the experimental risk parameters and the geometric parameters. The simulation risk value was 0.693.

There existed a large difference between the experimental and simulation results.

5.2.4 Error analysis

Contact resistance and dust appear the two main elements affecting the experimental results. This means the data logger may not be able to detect significant decrease of resistance given a whisker dropping in the conductor area.

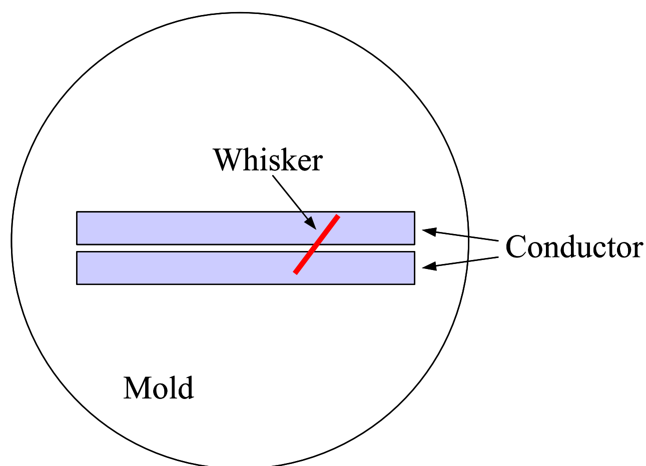

Figure 5.6 Test design for contact resistance

A simple testing vehicle was designed to test the influence of contact resistance. Similar to the experimental set for simulating bridging failure risk caused by fixed whiskers as shown in Figure 5.2, two coupons, with bright tin plated over brass, were paired together and separated by two 75-micron isolative Kapton films at each side. Then this set was potted with resign and resign hardener. The potted sample was polished to make the two coupon and the mold in the same plane.

Two tests using different conductors to study the influence of contact resistance. First tests were conducted using broken zinc whiskers. Originally, the

resistance between the two coupons is infinite. A whisker was laid on the two coupons, as illustrated in Figure 5.6. The ohm-meter still indicated infinite resistance, which means no electrical short occurs. Four tests have been conducted for zinc whiskers. Each time the same phenomenon, infinite resistance, was observed. However, the resistance dropped significantly down to the range of 5 to 10 ohms when Scotch tapes were laid on the whiskers to make them fully contact the conductors.

The second test was conducted using carbon fibers for 10 times. Similar to the first test, the resistance was infinity when a carbon fiber was laid on the surfaces of the two conductors without loading. The resistance dropped significant down to the range of 10 to 20 ohms when Scotch tapes were used to make the carbon fibers fully contact the conductor surface.

Based on the test results, it can be seen that a bridging electrical short may not occur due to contact resistance given a whisker physically bridges adjacent conductors. Studies on the probability of occurrence of an electrical short, given a whisker bridging the adjacent exposed conductors, are suggested to conduct.

Dusts may be another reason to prevent a zinc whisker from causing an electrical short in the experiment. Average dust density was more than 1000 #/cm^2, which was much larger than the whisker density. Whiskers may drop into the conductor area but on top of dust, which prevent a whisker from touching the conductor surfaces.

Chapter 6 Conclusions and Summary

The risk assessment algorithm developed in this dissertation is applicable to approach the bridging failure risk posed by (tin) whiskers to the pure tin or high tin alloy finished electronic products for the electronics industry. Though the algorithm to assess the bridging risk posed by broken free whiskers has errors, mainly caused by contact resistance, the concept and procedure are reasonable.

Tin whisker bridging risks are categorized into risk introduced by fixed whiskers and risk introduced broken free whiskers. The algorithm to assess these two categories of risks is different. The risk parameters for the two categories of risks are also different.

It is found that distributions are good ways to describe tin whisker growth and performance. In this study, lognormal, normal and step-wise distributions are applied to quantify whisker length, density and growth angle. The distributions are functions of time since the parameters of the distribution change with time when whiskers are growing.

Growth rates of whisker mean length and average density are calculated based on the obtained whisker growth information. Growth rates decrease with time if whisker growth is approaching the saturation point where whiskers cease growth. For this case, the latest growth rates can be used to predict whisker growth in mean length and density. If whisker growth is not approaching the saturation point, interpolation technique can be used, based on the obtain growth trend, to predict whisker growth. If there is no apparent trend, average growth rates can be used to predict.

It should be pointed out that tin whisker bridging failure risk is the joint results of the risk parameters. In the previous studies, especially for bridging risk of fixed whiskers, maximum whiskers in length was the only criterion for risk acceptance level. But maximum whisker length itself may not represent the real risk and this was a qualitative analysis.

The experiments can be used to simulate the bridging failure risks caused by fixed and broken free whiskers, and collect whisker growth and characteristic data; whereas the previous experiments focused on tin whiskering propensity. Resistance is selected as the monitoring parameter to examine bridging. In order to conduct the in-situ monitoring, data loggers are suggested to use in the experiment of simulating broken free whisker bridging failure.

Chapter 7 Contributions and Recommendations

The contributions of this research work are summarized. Recommendations to the future work are proposed and discussed.

7.1 Contributions of This Work

Contributions of this work include:

1. Probabilistic method was applied to characterize whisker growth
2. Proposed a method to predict whisker growth
3. Developed a tin whisker bridging risk assessment methodology, which provides the electronics industry a practical way to assess and predict tin whisker bridging risk quantitatively for the pure tin and high tin lead-free alloy finished products.
4. Designed and conducted the experiments to simulate tin whisker bridging failure.

In this study, whisker density, length and growth angle were quantified in terms of distributions. Distributions represent the group whisker growth. This is because 1) distribution reflect whisker group-growth trend; and 2) distributions contains the uncertainties in the measurement. As a population, individual whiskers have different incubation period and growth rate; this make it impractical to trace whisker growth for the individual whiskers. Also, bridging risk introduced by whiskers is the result of the whole group but not several individual whiskers. Distributions can describe this characterization of the group-whisker-growth. There

exist uncertainties in measuring whisker density, length and growth angle. Distributions reflect the measurement uncertainties in the process.

Though compressive stresses appear the driving forces of whisker growth, no accepted model and accelerated factors available to describe and predict whisker growth as a function of the driving forces. In this study, the known whisker growth trends were used to predict whisker group-growth. Based on this, tin whisker bridging risk can be predicted.

The algorithm assesses tin whisker bridging risk quantitatively; whereas the previous studies were only qualitative analysis. Monte Carlo technique was applied to sample whiskers and quantify the bridging risk as a function of time. This algorithm is applicable to assess tin whisker bridging failure risk for the electronics industry.

The experiments were designed to simulate the bridging failure risk caused by fixed and broken free whiskers; whereas the previous experiments only focused on tin whiskering propensity. Method of data collection for broken free whiskers is provided in the experiment design. It was found experimentally that contact resistance was the main reason to prevent an electrical short from occurring given a whisker dropping into the exposed conductor area.

7.2 Recommendations for the Future Work

Recommendations are proposed to design the dynamic free risk experiment and develop risk assessment algorithms for arcing and plasma risk and contamination risk.

7.2.1 Probability of occurrence of an electrical short

The algorithm provides a simulation answer to the bridging failure risk caused by broken free whiskers. However, experiments showed that there existed a larger difference between the simulation and experimental results. Contact resistance has been considered the main reason and proven by the testing results.

In order to obtain a more accurate simulation answer, it is recommended to quantify the probability of occurrence of an electrical short given a whisker bridging adjacent exposed conductors physically. This number will be used as an input data to the algorithm to correct the final bridging simulation risk.

7.2.2 Bridging risk simulation on a real electronic system

As the first step to simulate the bridging risk caused by broken free whiskers, non-air-exchange experiment was designed, which has been discussed in Chapter 5. "Air-exchange" here refers to airflow flowing into and venting out the system. For an electronic product, such as a desktop computer, air is pushed by a fan into the control volume and then vents out. Whiskers can float with air into the computer and can also escape out of the computer with air.

Turbulent airflow is generated inside the control volume when air is push by a fan in the control volume. This results in the movement tacks of broken free whiskers complex. Probability of a whisker dropping in the conductor area does not follow uniform distribution. The floor of the control volume can be divided into several zones. In each zone, whiskers deposition is uniformly. For example, as shown in Figure 7.1, the floor of the control volume can be divided into six zones.

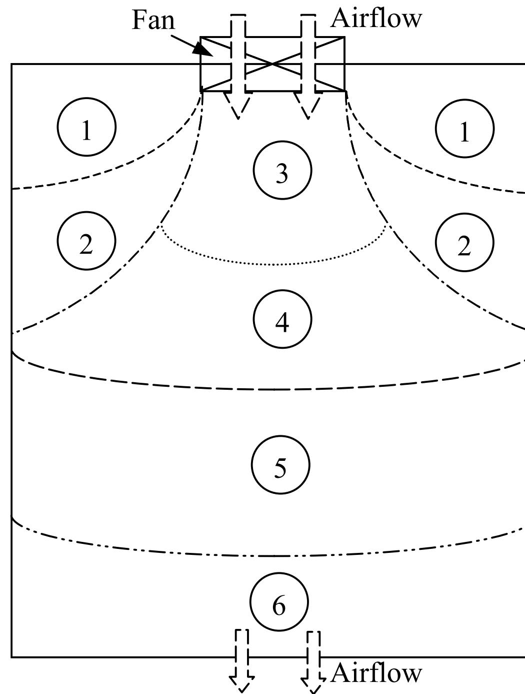

Figure 7.1 Whisker deposition zones

The methods, described in Chapter 5, to measure whisker density, length and deposition angle can also be applied to delineate the zones and collect data. By measuring whisker number in each cell, whisker number distribution on the floor can be quantified. Area of each zone is the sum of the area of the cells with similar density. The probability of a whisker dropping on the exposed conductors is the ratio of the conductor and zone area given this whisker falling in the zone.

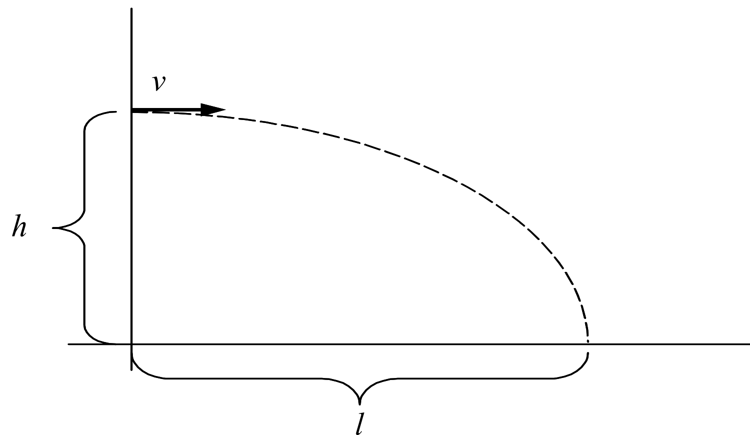

Figure 7.2 Maximum distance a whisker can reach

It is important to locate the zone where maximum percentage of whiskers deposit since the exposed conductors in this zone have the highest bridging risk. If airflow entering the control is laminar flow, the horizontal distance from the fan to the deposition site can be estimated by

$$\begin{cases} h = \frac{1}{2} \cdot g \cdot t^2 \\ l = v \cdot t \end{cases} \qquad (7.1)$$

where h is the perpendicular height from center of the fan to the floor of the control volume, g is gravity, t is time, l is the horizontal distance, and v is the whisker velocity entering the control volume. The physical procedure is shown in Figure 7.2. Zones near the site with distance l should have the largest number of deposited whiskers.

For turbulent airflow, equation 7.1 cannot be applied; but can be used as a reference to estimate the location of the zones having largest fraction of deposited whiskers. The real location of the zones can be detected by experiment as discussed in Chapter 5. By comparing the detected results to the results calculated by equation 7.1, the deviation of equation 7.1 can be obtained.

A key factor to this experiment is the quantity of broken free whiskers. It is critical to find a way to grow whiskers rapidly with large density and length. Chen et al [9] reported rapid whisker growth on electrodeposited tin-manganese alloy coatings. This growth was unique from the previously reported whisker growth on either pure tin or other tin-based alloy electrodeposits. The incubation period was as short as a few hours, followed by a spectacularly rapid and profuse growth. Chen's procedure may be applied to grow whiskers. Then the whiskers can be harvested, broken from the tin-manganese surfaces as broken free whiskers for the experiment.

7.2.3 Risk assessment algorithm development to quantify the other two risks

There are three types of potential risks posed by tin whiskers. Bridging failure risk assessment algorithm is developed in this study. The concepts of the algorithm are also applicable to assess risks from arcing and plasma, and contamination.

Arcing and plasma may occur when a whisker bridges two conductors and melts open with the applied electrical current and voltage large enough. Both fixed and free whiskers can cause arcing and plasma. Similar to bridging shorts, arcing and plasma also have fixed and free risk. The procedures of the algorithms for fixed and free risk can be applied to quantify arcing and plasma risk; but the failure criteria and the relevant parameters can be different.

Contamination is caused by free whiskers. The free risk algorithm can be borrowed to assess contamination risk. But the failure criteria can be different.

Bibliography

[1] S. M. Arnold, "The Growth and Properties of Metal Whiskers", *Proceedings of 43rd Annual Convention of the American Electroplater's Society*, pp. 26-31, 1956.

[2] S. M. Arnold, "The Growth of Metal Whiskers on Electrical Components", *Proceedings of the IEEE Electronic Component Conference,* pp. 75-82, 1959.

[3] S. M. Arnold, "Repressing the Growth of Tin Whiskers", *Plating,* Vol. 53, No. 1, pp. 96-99, January 1966.

[4] I. Boguslavsky and P. Bush, "Recrystallization Principles Applied to Whisker Growth in Tin", *Proceedings of IPC/SMEMA Council APEX2003*, pp. S12-4-1~S12-4-10, March 2003.

[5] B. L. Bowerman and R. T. O'Connell, Forecasting and Time Series: An Applied Approach, Duxbury Press, 3rd Edition, 1993.

[6] S. C. Britton, "Spontaneous Growth of Whiskers on Tin Coatings: 20 Years of Observation", *Transactions of the Institute of Metal Finishes*, Vol. 52, pp. 95-102, 1974.

[7] J. A. Brusse, "Tin Whisker Observations on Pure Tin-plated Ceramic Chip Capacitors", *AESF SUR/FIN Proceedings*, pp. 45-61, Orland, June 2002.

[8] J. A. Brusse, G.. Ewell, and J. P. Siplon, "Tin Whiskers: Attributes and Mitigation", *Proceedings of 22nd Capacitor and Resistor Technology Symposium,* pp. 67-80, March 25-29,2002.

[9] K. Chen and G. D. Wilcox, "Observations of the spontaneous growth of tin

whiskers on tin-manganese alloy electrodeposits", *Physical Review Letters*, vol.94, no.6, 18 Feb. 2005.

[10] H. L. Cobb, "Cadmium Whiskers", *Monthly Review of American Electroplaters Society*, Vol. 33, No. 28, pp.28-30, January 1946.

[11] K.G.. Compton, A. Mendizza, and S. M. Arnold, "Filamentary Growths on Metal Surfaces-Whiskers", *Corrosion*, Vol. 7, No. 10, pp. 327-334, October 1951.

[12] DATAPLOT Reference Manual, March 26, 1997, [Online] Available: http://www.itl.nist.gov/div898/software/dataplot/refman2/auxillar/tnrcdf.pdf.

[13] Department of Health, Education, and Welfare Public Health Service Drug Administration, "ITG Subject: Tin Whiskers-Problems, Causes, and Solutions", *Report No. 42*, [Online] Available: http://www.fda.gov/ora/inspect_ref/itg/itg42.html, June 2004.

[14] G. Davy, Northrop Grumman Electronic Systems, "Relay Failure Caused by Tin Whiskers", [Online]. Available: http://nepp.nasa.gov/whisker/reference/tech_papers/davy2002-relay-failure-caused-by-tin-whiskers.pdf, June 2004.

[15] M. Dittes, P. Oberndorff, and L. Petit, "Tin Whisker Formation-Results, Test Methods, and Countermeasures", *Proceedings of 53rd Electronic Components and Technology Conference*, pp. 822-826, May 27-30, 2003.

[16] B. D. Dunn, "Whisker Formation on Electronic Materials", *Circuit World*, Vol. 2, No. 4, pp. 32-40, 1976.

[17] B. D. Dunn, “A Laboratory Study on Tin Whisker Growth”, *European Space Agency STR-223,* pp. 1-50, September 1987.

[18] B. D. Dunn, “Mechanical and Electrical Characteristics of Tin Whiskers with Special Reference to Spacecraft Systems”, *European Space Agency*, 1988.

[19] Dupont, Kapton polyimide film, [Online] Available: http://www.dupont.com/kapton/general/H-38492-2.pdf, May 2005.

[20] W. C. Ellis, D. F. Gibbons, and R. C. Treuting, “Growth and Perfection of Crystals”, John Wiley, New York, 1958, pp. 102-120.

[21] J. D. Eshelby, “A Tentative Theory of Metallic Whisker Growth”, *Physics Review*, 91, pp. 755-756, 1953.

[22] European Union, “DIRECTIVE 2002/96/EC OF THE EUROPEAN PARLIAMENT AND OF THE COUNCIL of 27 January 2003 on waste electrical and electronic equipment (WEEE)”, *Official Journal of the European Union*, pp. L37/24-38, [Online] Available: http://europa.eu.int/eur-lex/pri/en/oj/dat/2003/l_037/l_03720030213en00240038.pdf.

[23] T. Fang, Michael Osterman, and Michael Pecht, “A Tin Whisker Risk Assessment Algorithm”, t*he 38th Annual IMAPS Symposium,* Philadelphia, Accepted for Publication on April 8th, 2005.

[24] T. Fang, Michael Osterman, and Michael Pecht, “Statistical Analysis of Tin Whisker Growth”, *Microelectronics Reliability*, Accepted for Publication on May 9th, 2005.

[25] F. C. Farnk, “On Tin Whiskers”, *Philosophical Magazine,* Vol. 44, pp. 854-860, August 1953.

[26] R. M. Fisher, L. S. Darken, and K. G. Carroll, “Accelerated Growth of Tin Whiskers”, *Acta Metallurgica*, Vol. 2, No. 3, pp. 368-372, May 1954.

[27] J. Franks, “Growth of Whiskers in the Solid Phase”, *Acta Metallurgica*, Vol. 6, No. 2, pp. 103-109, February 1958.

[28] N. Furuta and K. Hamamura, “Growth Mechanisms of Proper Tin-Whisker”, *Japanese Journal of Applied Physics*, Vol. 9, No. 12, pp. 1404-1410, December 1, 1969.

[29] S. Ganesan and M. Pecht, Lead-free Electronics, 2004 Edition, CALCE EPSC Press, University of Maryland, College Park, MD.

[30] G. T. Galyon and R. Gedney, “Avoiding Tin Whisker Reliability Problems”, *Circuits Assembly*, pp.26-31, Aug. 2004.

[31] V. K. Glazunova, and N. T. Kudryavtsev, “An Investigation of the Conditions of Spontaneous Growth of Filiform Crystals on Electrodeposit Coatings”, *Tranlated from Zhurnal Prikladnoi,* Vol. 36, No. 3, pp. 543-550, March 1963.

[32] P. Harri, “The Growth of Tin Whiskers”, *International Tin Research Institute (ITRI)*, Publication No. 734, 1994.

[33] R. D. Hilty and N. Corman, “Tin Whisker Reliability Assessment by Monte Carlo Simulation”, Tyco Electronics, [Online] Available: http://www.tycoelectronics.com/environment/leadfree/pdf/TE_IPCJEDEC_Hilty_Corman_WhiskerMonteCarlo_paper.pdf.

[34] HyperStat Online Contents, [Online] Available: http://davidmlane.com/hyperstat/A14043.html, May 2005.

[35] JEDEC Solid State Technology Association, “JEDEC Annouces Lead-free Definition”, [Online] Available: http://www.jedec.org/Home/press/leadfreePR.pdf, Sept. 2002.

[36] S. E. Koonce and S. M. Arnold, “Metal Whiskers”, *Journal of Applied Physics (letters to the editor),* Vol. 25, No. 1, pp. 134-135, 1954.

[37] B. Z. Lee and D. N. Lee, “Spontaneous Growth Mechanism of Tin Whiskers”, *Acta Materials*, Vol. 46, No. 10, pp.3701-3714, 1998.

[38] J. Chang-Bing Lee, Y-L. Yao, F-Y. Chiang, P. J. Zheng, C. C. Liao, and Y. S. Chou, “Characterization Study of Lead-free SnCu Plated Packages”, *Proceedings of IEEE Electronic Component and Technology Conference*, pp. 1238-1245, 2002.

[39] H. Leidecker, and J. S. Kadesch, “Effects of Uralane Conformal Coating on Tin Whisker Growth”, *Proceedings of IMAPS Nordic, the 37th IMAPS Nordic Annual Conference,* pp. 108-116, 10-13 September 2000.

[40] A. Leon-Garcia, Probability and Random Processes for Electrical Engineering”, 2nd Edition, Addison Weley, 1998.

[41] U. Lindborg, “A Model for the Spontaneous Growth of Zn, Cadmium, and Tin Whiskers”, *Acta Metallurgica,* Vol. 24, No. 2, pp. 181-186, February 1976.

[42] H. Livingston, “Reducing the Risk of Tin Whisker-Induced Failures in Electronic Equipment”, BAE SYSTEMS Information and Electronic Warfare

Systems, Dec. 2003.

[43] M.E. McDowell, "Tin Whiskers: A Case Study, (USAF)", *Aerospace Applications Conference,* pp. 207 -215, 1993.

[44] NASA, “Parts Advisory: Tin Whiskers”, *NA-044,* [Online] Available: http://nepp.nasa.gov/npsl/Prohibited/na-044.pdf, June 2004.

[45] NASA GSFC, "Basic Information Regarding Tin Whiskers", [Online] Available: http://nepp.nasa.gov/whisker.

[46] NASA Goddard Space Flight Center, Tin Whisker (and Other Metal Whisker) Homepage, [Online] Available: http://nepp.nasa.gov/whisker, April 2005.

[47] NEMI, “Interim Recommendations of Lead-free Finishes for Components Used in High-Reliability Products”, *Report of the National Electronics Manufacturing Initiatives (NEMI) Tin Whisker User Group,* [Online] Available: ftp://nemi.org/webdownload/projects/ese/TW_User_Group_position0304.pdf, June 2004.

[48] NEMI, “NEMI’s Lead-free Asembly Project Reports Latest Results at APEX 2002”, [Online] Available: http://www.nemi.org/Newsroom/PR/PR012102b.html, Sept. 2002.

[49] S. Okada, S. Higuchi, and T. Ando, “Field Reliability Estimation of Tin Whiskers Generated by Thermal-Cycling Stress”, Murata Manufacturing Corporation, Ltd, 2003.

[50] M. Osterman, "Mitigation Strategies for Tin Whiskers", CALCE EPSC, University of Maryland, [Online] Available:

http://www.calce.umd.edu/lead-free/tin-whiskers/TINWHISKERMITIGATION.pdf, Aug. 2002.

[51] M. Osterman, "Tin Whisker Risks", *White Paper of CALCE EPSC,* Revision 1, 19 June 2002, [Online] Available: http://www.calce.umd.edu/lead-free/tin-whiskers/TINWHISKERRISKS.pdf.

[52] M. O. Peach, "Mechanism of Growth of Whiskers on Cadmium", *Journal of Applied Physics (letters to the editor)*, Vol. 23, No. 12, pp. 1401-1403, 1952.

[53] D. Pinsky, Raytheon, RAL, [Online] Available: https://www.reliabilityanalysislab.com/tl_dp_0312_TinWhiskerRiskAssessmentAlgorithm.asp, Mar. 2005.

[54] D. Pinsky and E. Lambert, "Tin Whisker Risk Mitigation for High-Reliability Systems Integrators and Designers", *Technical Report of Raytheon,* March 2004, [Online] Available: http://www.reliabilityanalysislab.com/tl_dp_0403_TinWhiskerRiskMitigation.asp, (17 July 2004).

[55] D. Pinsky, M. Osterman, and S. Ganesan, "Tin Whiskering Risk Factors", *IEEE Transactions on Components and Packaging Technologies*, Vol. 27, No. 2, pp. 427 – 431, June 2004.

[56] N. A. J. Sabbagh and H. J. McQueen, "Tin Whiskers: Causes and Remedies", *Metal Finishing,* VOL. pp. 27-31, March 1975.

[57] H. Schneider, Truncated and Censored Samples from Normal Populations, New York: M. Dekker, 1986.

[58] J. Smetana, “NEMI Tin Whisker User Group – Tin Whisker Acceptance Test Requirements”, *NEMI Tin Whisker Workshop*, June 1-2, 2004, Las Vegas, NV.

[59] G. W. Stupian, “Tin Whiskers in Electronic Circuits”, *Aerospace Report*, No. TR-92 (2925)-7, pp. 1-21, December 20, 1992.

[60] K.N. Tu, “Interdiffusion and Reaction in Bimetallic Cu-Sn Thin Films”, *Acta Metallurgica,* Vol. 21, No. 4, pp. 347-354, April 1973.

[61] K.N. Tu, “Irreversible Processed of Spontaneous Whisker Growth in Bimetallic Cu-Sn Thin Film Reactions”, *Physics Review B,* Vol. 49, No. 3, pp. 2030-2034, January 1994.

[62] Tyco Electronics, 2004, “Keeping Tin Solderable”, [Online] Available: http://www.amp.com/products/technology/articles/dd47a.stm, July 9, 2000.

[63] K. Whitlaw, A. Egli, and M. Toben, “Preventing Whiskers in Electrodeposited Tin for Semiconductor Lead Frame Applications”, *Proceedings of the IPC International Conference on Lead-Free Electronics,* Brussels, June 2003.

[64] T. Woodrow, B. Rollins, P. Nalley, and B. Ogden, “Tin Whisker Mitigation Study: Phase 1: Evaluation of Environments for Growing Tin Whiskers”, *Draft report*, released on August 2003, [Online] Available: http://www.calce.umd.edu/lead-free/tin-whiskers/restricted/PhaseIDraft2.pdf, June 2004.

[65] C. Xu, Y. Zhang, C. Fan, J. Abys, L. Hopkins, and F. Stevie, “Understanding Whisker Phenomenon, Driving Force for the Whisker Formation”, *Proceedings of IPC SMEMA Council APEX 2002*, pp. S06-2-1~S06-2-6,

January 2002.

[66] Y. Zhang, C. Fan, C. Xu, O. Khaselev, and J. A. Abys, “Tin Whisker Growth – Substrate Effect: Understanding CTE Mismatch and IMC formation”, *CircuiTree*, June 2004.

[67] Y. Zhang, C. Xu, C. Fan, J. Abys, and A. Vysotskaya, "Understanding Whisker Phenomenon: Whisker Index and Tin/Copper, Tin/Nickel Interface", *Proceedings of the IPC SMEMA Council APEX*, pp. S06-1-1 thru S06-1-11, January 2000.